STING is a common driver of type I interferon responses to diverse bacteria in macrophages

Stephanie A. Ragland and Jonathan C. Kagan*

Division of Gastroenterology, Boston Children's Hospital and Harvard Medical School, 300 Longwood Avenue, Boston, MA 02115, USA

*Correspondence: jonathan.kagan@childrens.harvard.edu

Keywords: macrophage, phagosome, Toll-like receptor, MyD88, TRIF, type I interferon, cGAS, STING, cyclic dinucleotides, lipopolysaccharide, *Staphylococcus aureus*, *Staphylococcus epidermidis*, *Listeria innocua*, *Lactococcus lactis*, *L. plantarum*, *Micrococcus luteus*, *Enterococcus faecalis, Bacillus subtilis*, *Escherichia coli*, *Neisseria perflava*, *Yersinia pseudotuberculosis*, *Bacteroides fragilis*, *Bacteroides thetaiotaomicron*

Abstract

Pattern recognition receptors (PRRs) of the innate immune system detect conserved bacterial molecules, termed pathogen-associated molecular patterns (PAMPs). Toll-like receptors (TLRs) are considered the only PRRs that can detect all bacteria, regardless of virulence potential. These PRRs survey PAMPs in the extracellular and phagosomal space, where most bacteria are found. Other PRR families mostly consist of proteins that are localized to the cytosol of immune cells. Due to the membranous barrier of phagosomes, cytosolic PRRs should be restricted from accessing extracellular or phagosomal bacteria and are generally considered to detect pathogens that use virulence factors to disrupt membranes. Despite this rationale, disparate reports suggest that some non-pathogenic, phagosomal bacteria stimulate cytosolic PRRs. In this work, we tested the null hypothesis that TLRs are the only PRRs that commonly detect bacteria. We found that diverse bacteria, regardless of their pathogenicity, stimulated type I interferon (IFN-I) responses in macrophages. While optimal IFN-I responses to Gram-negative bacteria required TLRs, all bacteria stimulated IFN-I through the cytosolic PRR STING. Synthetic biology-based engineering of bacteria to produce distinct STING stimulatory cyclic dinucleotides (CDNs) revealed that CDN abundance within phagosomes is a key determinant of IFN-I induction by macrophages. The STING pathway therefore joins the TLRs as a common driver of innate immune responses to bacterial encounters.

Introduction

Mammalian cells utilize pattern recognition receptors (PRRs) to detect infections via interactions with bacterial molecules known as pathogen-associated molecular patterns (PAMPs). Several PRR families detect bacterial products, including the Toll-like receptors (TLRs), RIG-I like receptors (RLRs), and nucleotide-binding domain leucine-rich repeat containing proteins (NLRs), as well as a pathway involving two PRRs, the enzyme cyclic GMP-AMP synthase (cGAS) and stimulator of interferon genes (STING) [1]. In the case of cGAS and STING, both detect bacterial products (DNA and cyclic dinucleotides (CDNs), respectively); however, because cGAS produces a CDN upon detection of DNA that is operationally analogous to bacterial CDNs, cGAS activation feeds into STING-dependent immunity [2, 3].

Each PRR family is structurally distinct from the others, yet they are conceptually connected by the common ability to link PAMP detection to the production of cytokines and other factors that promote defense and adaptive immunity [4-6]. Among the PRR families, TLRs are considered the best equipped to operate as sensors of any bacterial encounter. This prime function of TLRs can be explained by the distinct subcellular positioning of PRRs [7]. TLRs are transmembrane proteins whose PAMP-recognition domains survey the extracellular and the intra-endosomal spaces. In contrast, the PAMP-recognition domains of RLRs, NLRs, cGAS, and STING are positioned in the cytosolic space and are therefore separated from extracellular and phagosomal bacteria by a lipid bilayer. For this reason, whereas TLRs are often considered generic sensory proteins, the other aforementioned PRRs detect only select bacteria [8, 9]. These select bacteria are typically pathogens that encode virulence factors that disrupt membranes, such as exotoxins and types 3 and 4 secretion systems [9, 10].

Despite this general view, examples exist where non-virulent bacteria stimulate cytosolic PRRs (reviewed in [10]). For instance, separate studies have revealed that non-virulent strains of *Legionella pneumophila* and *Pseudomonas aeruginosa*, as well as non-pathogenic *Escherichia coli*, *Mycobacterium smegmatis*, and *Listeria innocua* are capable of stimulating cytosolic PRRs [11-14]. However, perhaps due to the study of separate bacteria (and PRR pathways) in these prior studies, the principles of host-bacteria interactions remain focused on the prevailing view – that TLRs are the only PRR family that commonly detects bacterial encounters. Herein, we sought to test the null hypothesis that TLRs are the only common means by which cells detect bacteria. To this end, we studied immune responses to a diverse panel of non-pathogenic and pathogenic bacteria. With the

exception of bacteria that produce TLR4-stimulatory lipopolysaccharides (LPS), most bacteria we examined stimulated TLR-independent type I interferon (IFN-I) cytokine responses via the cytosolic PRR STING. Diverse species of bacteria stimulated STING directly, or indirectly by activating the upstream PRR cGAS. By increasing intra-bacterial CDN abundance through synthetic biology, we converted *E. coli* from a direct activator of cGAS to a direct activator of STING. These collective findings establish that TLRs are not the only PRRs that commonly operate to detect bacteria. Instead, STING is a common participant in host-bacteria interactions, regardless of their virulence potential.

Results

TLR-dependent and -independent IFN-I responses by macrophages upon diverse bacterial encounters

To identify common innate immune activities in macrophages, we assembled a panel of 8 Gram-positive bacteria (*Staphylococcus aureus*, *Staphylococcus epidermidis*, *L. innocua*, *Lactococcus lactis*, *Lactobacillus plantarum*, *Micrococcus luteus*, *Enterococcus faecalis, Bacillus subtilis*) and 5 Gram-negative bacteria (*E. coli*, *Neisseria perflava*, *Yersinia pseudotuberculosis*, *Bacteroides fragilis*, and *Bacteroides thetaiotaomicron*) (**Supplemental Table 1**). These bacteria represent pathogens and non-pathogens [15-26], but all should reside primarily in phagosomes. We performed synchronous, side-by-side infections of Wild-type (WT) murine primary bone marrow-derived macrophages (BMDMs) and measured the production of cytokines that are regulated by the innate immune transcription factors NF-κB and interferon regulatory factors (IRFs). NF-κB activities were assessed by macrophage production of the pro-inflammatory cytokine TNFα. IRF activities were assessed by macrophage production of the IFN-I cytokine IFNβ, as well as IFN-I activities by measuring IFN stimulated gene (ISG) expression. At 4 and 24 hrs post-exposure, all bacteria examined were found to induce secretion of comparable amounts of TNFα (**Supplemental Fig. 1A**).

In contrast to TNFα, distinct patterns of IFN-I responses were observed. By measuring secretion of IFNβ and the ISG product IP-10 (also known as CXCL10), we identified three distinct classes of bacteria and IFN-I responses (**Supplemental Fig. 1B, C**). One class induced early (*i.e.,* 4 hrs) IFN-I responses to bacteria that matched the IFN-I response kinetics and magnitude of *E. coli* LPS. This class included the Gram-negatives *E. coli*, *N. perflava*, *Y. pseudotuberculosis*, and the Gram-positive *S. aureus*. A second class of bacteria also induced IFN-I responses comparable to those elicited by LPS, but with delayed kinetics (*i.e.,* 24 hrs). This class included the Gram-positives *S. epidermidis*, *L. innocua*, *L. lactis*, *L. plantarum*, and *M. luteus*. Finally, the third

class of bacteria were poor IFN-I inducers at either timepoint examined and included the Gram-positives *E. faecalis* and *B. subtilis* and the Gram-negatives *B. fragilis* and *B. thetaiotaomicron*.

Similar trends in the kinetics and magnitude of IFNβ and IP-10 were observed in immortalized murine bone marrow macrophages (iBMMs) exposed to bacteria, and TNFα levels produced by iBMMs were similar to all bacteria at both timepoints (**Fig. 1A-C**, black bars). To corroborate these findings, we examined additional IFN-I activities. IFNβ signaling through the IFN-α/β receptor (IFNAR) activates STAT1, which promotes transcription of ISGs [27]. Thus, we examined activated STAT1 (*i.e.,* STAT1 phosphorylated at Y701, pSTAT1), as well as the ISG product Viperin by immunoblot in iBMMs. Both of these IFN-I readouts were increased in cells exposed for 4 hrs to the Gram-negatives *E. coli*, *N. perflava*, and *Y. pseudotuberculosis* and the Gram-positive *S. aureus* (**Fig. 1D**, left panel). All other bacteria examined failed to stimulate pSTAT1 or Viperin production at this early timepoint, compared with uninfected cells (**Fig. 1D**, left panel). However, by 24 hrs, virtually all bacteria examined induced similar amounts of pSTAT1 and Viperin protein in iBMMs (**Fig. 1E**, left panel). As STAT1 itself is an ISG product [28], we also observed increased total STAT1 abundance to bacteria in iBMMs at 24 hrs, compared to uninfected cells (**Fig. 1E**, left panel). Taken together, several independent assays revealed that most Gram-negative and Gram-positive bacteria stimulate IFN-I responses in macrophages, although with distinct kinetics.

To determine the role of TLRs in macrophage responses to diverse bacteria, we employed iBMMs doubly deficient in the adaptor proteins MyD88 and TRIF. These cells are defective for all transcriptional responses that are normally induced by TLRs [4]. As expected, TLR ligands did not stimulate any detectable inflammatory activity in *Myd88$^{-/-}$Trif$^{-/-}$* iBMMs (**Supplemental Fig. 2**). These defective cellular responses included transcription of *ifnb1* and the ISG *rsad2,* which encodes the protein Viperin, as well as production of pSTAT1 and Viperin protein itself (**Supplemental Fig 2A-D**). In contrast, IFN-I responses to ligands for STING and NOD2 remained intact in *Myd88$^{-/-}$Trif$^{-/-}$* iBMMs (**Supplemental Fig 2A-D**). We found that exposure of *Myd88$^{-/-}$Trif$^{-/-}$* iBMMs to all bacteria we examined resulted in minimal secretion of TNFα across all timepoints (**Fig. 1A**, orange bars). Thus, a common response for macrophages exposed to bacteria is TLR-dependent secretion of TNFα.

After 4 hrs exposure to most bacteria, *ifnb1* and *rsad2* transcriptional responses were largely absent in *Myd88$^{-/-}$Trif$^{-/-}$* iBMMs, compared to wild type (WT) iBMMs (**Supplemental Fig. 3A, B**). IFNβ, IP-10, pSTAT1, and Viperin protein levels to most bacteria were also poorly detectable in *Myd88$^{-/-}$Trif$^{-/-}$* iBMMs (**Fig. 1B-C**, orange

bars and **Fig. 1D-E**). One exception was *S. aureus*, whose early stimulation of IFN-I responses was largely unaffected in iBMMs lacking MyD88 and TRIF (**Fig. 1**, **Supplemental Fig. 3**). Thus, TLR signaling is important for early IFN-I responses to most bacteria in macrophages. In contrast, by 24 hrs exposure, most bacteria stimulated *ifnb1* and *rsad2* transcriptional responses in WT and *Myd88*$^{-/-}$*Trif*$^{-/-}$ iBMMs (**Supplemental Fig. 3A, B**). Moreover, most bacteria stimulated secretion or production of the proteins IFNβ, IP-10, pSTAT1, STAT1, and Viperin in *Myd88*$^{-/-}$*Trif*$^{-/-}$ iBMMs after 24 hrs exposure, compared to uninfected cells (**Fig. 1B-C**, orange bars and **Fig. 1D-E**). While a multiplicity of infection (MOI) as low as 1 was sufficient for most bacteria to stimulate increased pSTAT1, total STAT1, and Viperin protein in WT iBMMs by 24 hrs, MOIs of 10 or higher were needed to stimulate similar IFN-I responses in *Myd88*$^{-/-}$*Trif*$^{-/-}$ iBMMs to several bacteria, especially Gram-negatives (**Supplemental Fig. 4**). Indeed, Gram-positive bacteria overall stimulated stronger TLR-independent IFN-I than Gram-negative bacteria (**Fig. 1**). IFN-I responses were not associated with host cell death as lactate dehydrogenase release, a marker for inflammatory cell death, did not correlate with IFN-I activities induced by the collection of bacteria examined (**Supplemental Fig. 5**). Taken together, these findings demonstrate that many bacteria stimulate TLR-independent IFN-I responses.

TLR-independent IFN-I responses to bacteria require a TBK1-IRF3-IFNAR signaling axis

We defined pathway features important for TLR-independent IFN-I signaling, using a refined group of our examined bacteria. These bacteria included *S. aureus*, *S. epidermidis, L. innocua*, and *Y. pseudotuberculosis*. To determine if phagocytosis was necessary for IFN-I production, we used the phagocytosis inhibitor cytochalasin D and measured early *ifnb1* transcriptional responses. At the time point examined (6 hrs), vehicle-treated *Myd88*$^{-/-}$*Trif*$^{-/-}$ iBMMs exposed to *S. aureus*, *S. epidermidis*, and *L. innocua* exhibited marked increases in *ifnb1* transcriptional responses, which were reduced upon treatment with cytochalasin D (**Fig. 2A**). Thus, phagocytosis of bacteria is a prerequisite for TLR-independent IFN-I. We next examined whether inactivation of bacteria via paraformaldehyde fixation alters TLR-independent IFN-I responses in macrophages. For *S. aureus* and *L. innocua*, *Myd88*$^{-/-}$*Trif*$^{-/-}$ iBMMs exposed to inactivated bacteria for 24 hrs exhibited strongly reduced pSTAT1, total STAT1, and Viperin protein levels, compared to live bacteria (**Supplemental Fig. 6A, C**). Consistent with a previous report [29], expression of the type 3 secretion system of *Y. pseudotuberculosis* was required for increased pSTAT1, total STAT1, and Viperin protein levels in *Myd88*$^{-/-}$*Trif*$^{-/-}$ iBMMs, a process that required bacterial viability (**Supplemental Fig. 6D**). In contrast, live and inactivated *S. epidermidis* stimulated

similar pSTAT1, total STAT1, and Viperin protein levels in *Myd88*$^{-/-}$*Trif*$^{-/-}$ iBMMs (**Supplemental Fig. 6B**). Thus, bacterial viability is not universally required for TLR-independent IFN-I responses.

We observed pSTAT1 in *Myd88*$^{-/-}$*Trif*$^{-/-}$ iBMMs exposed to bacteria (**Fig 1D, E**), suggesting that IFNAR signaling is active in response to bacteria. To examine whether IFNAR is required to produce TLR-independent ISG production, we used CRISPR/Cas9 to inactivate *ifnar1* in *Myd88*$^{-/-}$*Trif*$^{-/-}$ iBMMs. As expected, recombinant IFNβ protein was unable to elicit IP-10 protein from *Myd88*$^{-/-}$*Trif*$^{-/-}$*Ifnar1*$^{-/-}$ iBMMs (**Fig. 2B**, left). Upon exposure to bacteria, IP-10 protein abundance was also reduced in *Myd88*$^{-/-}$*Trif*$^{-/-}$*Ifnar1*$^{-/-}$ iBMMs, compared with *Myd88*$^{-/-}$*Trif*$^{-/-}$ iBMMs (**Fig. 2B**, left). *Myd88*$^{-/-}$*Trif*$^{-/-}$ and *Myd88*$^{-/-}$*Trif*$^{-/-}$*Ifnar1*$^{-/-}$ iBMMs exhibited a similar capacity to secrete IFNβ in response to bacteria (**Fig. 2B**, right). Thus, IFNAR is required for TLR-independent ISG production, but not IFNβ production, in response to bacterial encounters.

Most cytosolic PRRs signal through IRF3 to promote IFN-I transcription [9]. We found that exposure of *Myd88*$^{-/-}$*Trif*$^{-/-}$ iBMMs to bacteria resulted in increased abundance of activated IRF3 (*i.e.,* IRF3 phosphorylated at S396) (**Fig. 2C**). To determine if IRF3 is required for IFN-I responses to bacteria, we generated *irf3*-deficient *Myd88*$^{-/-}$*Trif*$^{-/-}$ iBMMs (**Fig. 2D** inset). Upon exposure to a CDN (a synthetic bacterial CDN analog 2'3'-c-di-AM(PS)2 (Rp, Rp)) that activates IRF3 via STING, *Myd88*$^{-/-}$*Trif*$^{-/-}$*Irf3*$^{-/-}$ iBMMs were defective for IP-10 secretion, compared to *Myd88*$^{-/-}$*Trif*$^{-/-}$ iBMMs (**Fig. 2D**). In contrast, IRF3 was dispensable for IP-10 production in response to recombinant IFNβ protein (**Fig. 2D**). We found that all bacteria examined were defective for inducing IP-10 secretion from *Myd88*$^{-/-}$*Trif*$^{-/-}$*Irf3*$^{-/-}$ iBMMs, indicating that IRF3 is required for TLR-independent IFN-I production to bacteria (**Fig. 2D**).

IRF3 is commonly activated by the kinase TBK1 [9]. We observed increased abundance of activated TBK1 (*i.e.,* TBK1 autophosphorylated at S172) in *Myd88*$^{-/-}$*Trif*$^{-/-}$ iBMMs exposed to bacteria (**Fig. 2E**). To examine if TBK1 is important for IFN-I responses to bacteria, we first used a specific TBK1 inhibitor, MRT67307. Compared to vehicle control, TBK1 inhibition in *Myd88*$^{-/-}$*Trif*$^{-/-}$ iBMMs resulted in reduced pSTAT1, total STAT1, and Viperin proteins levels upon exposure to CDN or all bacteria examined (**Supplemental Fig. 7**). We next generated *Tbk1*-deficient *Myd88*$^{-/-}$*Trif*$^{-/-}$ iBMMs (**Fig. 2F** inset) and found that *Myd88*$^{-/-}$*Trif*$^{-/-}$*Tbk1*$^{-/-}$ iBMMs produced significantly reduced IP-10 protein abundance upon exposure to CDN or bacteria, compared with *Myd88*$^{-/-}$*Trif*$^{-/-}$ iBMMs (**Fig. 2F**). Together, these data indicate that a common feature of the TLR-independent IFN-I response to phagocytosed bacteria is the dependence on a TBK1-IRF3-IFNAR signaling axis.

STING controls TLR-independent IFN-I responses to bacteria in macrophages

To determine which PRR is detecting bacteria, we examined proteins involved in activating TBK1-IRF3-IFNAR signaling. MAVS is an adaptor protein required to induce IRF3-dependent IFN-I responses downstream of the RLRs, RIG-I and MDA5, both of which detect microbial RNAs in the cytosol [9]. We therefore generated *Myd88*$^{-/-}$*Trif*$^{-/-}$*Mavs*$^{-/-}$ iBMMs (**Supplemental Fig. 8A** inset). *Mavs*-deficiency resulted in ablated IP-10 production upon exposure to Sendai Virus, a strong RIG-I agonist (**Supplemental Fig. 8A**). In contrast, *Myd88*$^{-/-}$*Trif*$^{-/-}$ and *Myd88*$^{-/-}$*Trif*$^{-/-}$*Mavs*$^{-/-}$ iBMMs secreted similar amounts of IP-10 upon exposure to CDN and all bacteria examined (**Supplemental Fig. 8A**). These data indicate that MAVS is not responsible for TLR-independent IFN-I to bacteria. The peptidoglycan sensor NOD2 reportedly signals through the RIP2 kinase to stimulate IFN-I responses via TBK1 and IRF3 [30]. We therefore generated *Myd88*$^{-/-}$*Trif*$^{-/-}$*Rip2*$^{-/-}$ iBMMs (**Supplemental Fig. 8B** inset) and found that compared to parental cells, *Rip2*-deficiency resulted in ablated IP-10 responses to the NOD2 agonist N-glycolyl-muramyl dipeptide (**Supplemental Fig. 8B**). Normal IP-10 responses to CDN were observed (**Supplemental Fig. 8B**). *Myd88*$^{-/-}$*Trif*$^{-/-}$*Rip2*$^{-/-}$ iBMMs exhibited modest reductions in IP-10 in response to bacterial treatments, compared to *Myd88*$^{-/-}$*Trif*$^{-/-}$ iBMMs (**Supplemental Fig. 8B**). To further examine the role of RIP2 during infection, we examined early *S. aureus* IFN-I responses and found that pTBK1, pSTAT1, and Viperin protein abundance was comparable between *Myd88*$^{-/-}$*Trif*$^{-/-}$ and *Myd88*$^{-/-}$*Trif*$^{-/-}$*Rip2*$^{-/-}$ iBMMs (**Supplemental Fig. 8C**). This finding suggests that RIP2 may contribute to sustained IFN-I responses but is not strictly required for initiation of these responses.

We next examined a role for STING. STING detects CDNs that are produced by bacteria (*e.g.,* 3'3-c-di-AMP, 3'3'-c-di-GMP, and 3'3-cGAMP). STING can also detect 2'3'-cGAMP, which is produced by DNA-bound cGAS [2, 3]. We observed that WT and *Myd88*$^{-/-}$*Trif*$^{-/-}$ iBMMs exposed to bacteria for 4 hrs exhibited increased amounts of activated STING (*i.e.,* STING phosphorylated at S365, pSTING) (**Fig. 3A**). Primary BMDMs also exhibited increased pSTING abundance upon exposure to bacteria (**Supplemental Fig. 9A**). We therefore generated *Myd88*$^{-/-}$*Trif*$^{-/-}$*Sting*$^{-/-}$ iBMMs (**Fig. 3B** inset) and found that *Myd88*$^{-/-}$*Trif*$^{-/-}$ and *Myd88*$^{-/-}$*Trif*$^{-/-}$*Sting*$^{-/-}$ iBMMs produced similar IP-10 secretion in response to Sendai Virus (**Fig. 3B**). In contrast, *Myd88*$^{-/-}$*Trif*$^{-/-}$*Sting*$^{-/-}$ iBMMs were defective for IP-10 secretion in response to agonists that directly (CDN) or indirectly (cytosolic DNA via cGAS) stimulate STING (**Fig. 3B**). Exposure of cells to every bacterial strain examined from our panel (*i.e.,* the Gram-positives *Staphylococcus aureus*, *Staphylococcus epidermidis*, *Listeria innocua*, *Lactococcus lactis*,

Lactobacillus plantarum, *Micrococcus luteus*, and *Enterococcus faecalis*, as well as the Gram-negatives *Escherichia coli*, *Neisseria perflava*, and *Yersinia pseudotuberculosis*) revealed an ablation of IP-10 secretion in *Myd88*$^{-/-}$*Trif*$^{-/-}$*Sting*$^{-/-}$ iBMMs, compared to *Myd88*$^{-/-}$*Trif*$^{-/-}$ iBMMs (**Fig. 3B**). IFNβ secretion was also reduced or below the level of detection in *Myd88*$^{-/-}$*Trif*$^{-/-}$*Sting*$^{-/-}$ iBMMs exposed to all bacteria, compared to *Myd88*$^{-/-}$*Trif*$^{-/-}$ iBMMs (**Supplemental Fig. 10A**). These data demonstrate that STING detects diverse Gram-positive and Gram-negative bacteria.

To examine the interplay between STING and TLR signaling, we next generated *Sting*$^{-/-}$ cells in an otherwise WT background (**Fig. 3C** inset). Compared to WT iBMMs, IP-10 and IFNβ secretion in *Sting*$^{-/-}$ iBMMs was defective in response to all Gram-positive bacteria examined (**Fig. 3C** and **Supplemental Fig. 10B**). In contrast, WT and *Sting*$^{-/-}$ iBMMs secreted similar amounts of IP-10 and IFNβ in response to the examined Gram-negative bacteria (**Fig. 3C** and **Supplemental Fig. 10B**). The H-151 STING inhibitor [31] reduced IP-10 secretion from WT iBMMs to Gram-positive, but not Gram-negative, bacteria (**Supplemental Fig. 9B**, left). H-151 treatment of WT BMDMs also resulted in reduced pSTAT1, Viperin, and IP-10 protein abundance in response to Gram-positive bacteria, as compared to vehicle-treated cells (**Supplemental Fig. 9C, D**). Genetic deletion or inhibition of STING resulted in modest reductions in TNFα secretion (**Supplemental Fig. 9B, D** and **Supplemental Fig. 10A, B**). Importantly, the absence of STING in either WT or *Myd88*$^{-/-}$*Trif*$^{-/-}$ backgrounds failed to alter bacterial survival within macrophages (**Supplemental Fig. 11**), nor did absence of STING affect bacterial association with cells (**Supplemental Fig. 12**). Thus, STING is the principal PRR that directs IFN-I responses to Gram-positive bacteria, whereas Gram-negative bacteria are largely detected by TLRs to drive IFN-I responses.

Because STING can detect CDNs produced directly by bacteria or a CDN produced by cGAS [2, 3], we next examined the role for cGAS through generation of *Myd88*$^{-/-}$*Trif*$^{-/-}$*cGAS*$^{-/-}$ iBMMs (**Fig. 3D** inset). As expected, *Myd88*$^{-/-}$*Trif*$^{-/-}$*cGAS*$^{-/-}$ iBMMs were unresponsive to transfection with DNA, but not to pure CDN that bypasses cGAS to activate STING (**Fig. 3D** and **Supplemental Fig. 10C**). *Myd88*$^{-/-}$*Trif*$^{-/-}$*cGAS*$^{-/-}$ iBMMs were defective for IP-10 and IFNβ secretion in response to several of the examined Gram-positive and Gram-negative bacteria, as compared to *Myd88*$^{-/-}$*Trif*$^{-/-}$ iBMMs (**Fig. 3D** and **Supplemental Fig. 10C**). Notably, the Gram-positives *S. aureus*, *L. innocua*, and *L. lactis* stimulated IP-10 and IFNβ secretion from *Myd88*$^{-/-}$*Trif*$^{-/-}$*cGAS*$^{-/-}$ iBMMs (**Fig. 3D** and **Supplemental Fig. 10C**). Moreover, *S. aureus*, *L. innocua*, and *L. lactis*, but not other Gram-positive bacteria, also stimulated IP-10 and IFNβ production from WT iBMMs deficient for cGAS (**Fig. 3E** and **Supplemental Fig.**

10D). These data suggest that while STING is a common driver of IFN-I responses, cGAS-mediated detection is not.

CDN synthesis by bacteria is sufficient to induce cGAS-independent, STING-dependent IFN-I responses

For bacteria to stimulate cGAS-independent, STING-dependent IFN-I, they must synthesize their own STING-stimulatory CDNs. Several bacteria from our panel (*e.g., S. aureus*, *L. lactis*, *L. plantarum*, *E. faecalis*, and *E. coli*) are known to synthesize STING-stimulatory CDNs [32-36], yet not all of these bacteria stimulated cGAS-independent, STING-dependent IFN-I responses (**Fig. 3D**). Dissecting cGAS-independent STING responses to bacteria in a natural setting is complicated as manipulations of CDN abundance can impact bacterial viability and replication [37]. We therefore sought a synthetic biology approach to define the role of intrabacterial CDNs in STING agonism. We engineered non-pathogenic, laboratory *E. coli* strains to independently express three distinct CDN-synthesizing enzymes: *S. aureus* DacA which synthesizes 3'3'-c-di-AMP, *Vibrio cholerae* DncV which synthesizes 3'3'-cGAMP, or *Mus musculus* cGAS which synthesizes 2'3'-cGAMP [37]. As this bacterium does not produce these CDNs naturally, CDN alterations should have no impact on *E. coli* replication or viability.

We found that transgene expression in *E. coli* was relatively similar between each C-terminally 3xFLAG-tagged CDN synthase, with cGAS protein being the least abundant of the CDN synthases examined (**Supplemental Fig. 13A**). Infections with these bacteria revealed that the parent *E. coli* stimulated modest IP-10 protein levels in *Myd88$^{-/-}$Trif$^{-/-}$* iBMMs, by a cGAS- and STING-dependent process (**Fig. 4A**). *E. coli* producing DacA, DncV or cGAS stimulated profoundly increased IP-10 secretion from *Myd88$^{-/-}$Trif$^{-/-}$* iBMMs (**Fig. 4A**). Notably, *Myd88$^{-/-}$Trif$^{-/-}$* and *Myd88$^{-/-}$Trif$^{-/-}$cGAS$^{-/-}$* iBMMs secreted similar amounts of IP-10 to *E. coli* producing DacA, DncV or cGAS, whereas the absence of STING ablated IP-10 responses to these bacteria (**Fig. 4A**). Thus, heterologous expression of CDN-synthesizing enzymes is sufficient to convert *E. coli* from a direct agonist of cGAS to a direct STING agonist.

To understand the features important for direct STING activation, we used *E. coli::dacA*+ bacteria as a model for further dissection. WT and *Myd88$^{-/-}$Trif$^{-/-}$* iBMMs exposed to *E. coli::dacA*+ for 4 hrs resulted in increased detection of pSTING, pSTAT1, and Viperin abundance, compared to uninfected cells (**Fig. 4B**, left). By 24 hrs, total STING protein abundance was reduced upon exposure to *E. coli::dacA*+ or CDN in WT and *Myd88$^{-/-}$Trif$^{-/-}$* iBMMs, compared with uninfected cells (**Fig. 4B**, right). This decrease in STING abundance is

expected, since STING is degraded as a negative regulatory mechanism [2]. We note that infections with natural bacteria did not result in obvious STING degradation under similar conditions (**Fig. 3A**), suggesting that a larger proportion of total STING protein is activated by CDNs produced by engineered *E. coli*.

As pure CDNs added exogenously to macrophages can enter cells and stimulate STING [38, 39], it was possible that c-di-AMP is released from extracellular *E. coli::dacA*+ to activate IFN-I. To test this possibility, we harvested conditioned supernatants from *E. coli* and *E. coli::dacA*+ cultures. While *E. coli::dacA*+ bacteria stimulated IP-10 secretion from *Myd88*$^{-/-}$*Trif*$^{-/-}$*cGAS*$^{-/-}$ iBMMs, their conditioned supernatants failed to induce IP-10 secretion from these cells (**Supplemental Fig. 14**). This finding suggests that intracellular *E. coli::dacA*+ bacteria are the source of CDNs that stimulate STING. Consistent with this idea, preventing phagocytosis of *E. coli::dacA*+ by cytochalasin D treatment inhibited *ifnb1* transcription (**Fig. 4C**).

We next sought to manipulate c-di-AMP levels during infections with *E. coli::dacA*+. We first decreased *dacA* expression by altering the concentration of IPTG used for expression of *dacA* in *E. coli*. Decreasing IPTG concentrations resulted in a step-wise decrease in IP-10 secretion from *Myd88*$^{-/-}$*Trif*$^{-/-}$*cGAS*$^{-/-}$ iBMMs (**Supplemental Fig. 13B, C**). Furthermore, decreasing the MOI also resulted in a step-wise decrease in IP-10 secretion from *Myd88*$^{-/-}$*Trif*$^{-/-}$*cGAS*$^{-/-}$ iBMMs (**Fig. 4D**). Notably, an MOI as low as 0.1 induced robust IP-10 production (~25ng from ~10^6 cells) after 24 hrs exposure (**Fig. 4D**). To examine whether DacA enzymatic activity is important for cGAS-independent IFN-I responses, we generated *E. coli* expressing a mutant version of *dacA* where the codons for R208, H209, and R210 were swapped for codons encoding alanine. $DacA_{RHR_AAA}$ enzymes are unable to synthesize c-di-AMP [40]. *E. coli::dacA*$_{RHR_AAA}$ were defective for the induction of IP-10 secretion from *Myd88*$^{-/-}$*Trif*$^{-/-}$*cGAS*$^{-/-}$ iBMMs, as compared to *E. coli::dacA*$_{WT}$, despite equal expression of 3xFLAG-tagged proteins (**Fig. 4E**). Together these findings suggest that DacA enzymatic activity and protein levels define c-di-AMP levels and subsequent direct STING stimulation.

We found that paraformaldehyde-inactivated *S. aureus*, *L. innocua*, and *L. lactis* could not activate STING-dependent responses in iBMMs, as compared to their live counterparts (**Supplemental Fig. 6A, C, E**). Bacterial viability could be required to produce CDNs or viability could be required to damage phagosomes in a manner that delivers CDNs to STING. Our engineered *E. coli* presented an opportunity to dissociate these possibilities as expression of *dacA* should create a depot of intracellular c-di-AMP that would persist after bacterial killing. We found that live and inactivated *E. coli::dacA*+ stimulated secretion of similar amounts of IP-

10 from *Myd88*$^{-/-}$*Trif*$^{-/-}$*cGAS*$^{-/-}$ iBMMs (**Fig. 4F**). This finding rules out the possibility that *E. coli* are actively promoting STING activation through the damage or manipulation of phagosomes. Instead, the abundance of CDNs within phagosomes of dead bacteria is sufficient to stimulate STING-dependent responses.

Discussion

In this study, we found that diverse bacteria from 8 genera and 5 orders stimulated TLR-independent IFN-I responses. This TLR-independent IFN-I response universally required bacterial phagocytosis and a STING-TBK1-IRF3-IFNAR signaling axis. Our findings that many diverse, phagosomal bacteria stimulated STING and cGAS is puzzling because their ligands, CDNs and DNA, cannot passively diffuse across membranes.

How CDNs and DNA exit phagosomes is an open question. One possible explanation is that a small percentage of bacteria damage or escape the phagosome, and these infrequent events are therefore responsible for all the measured population-wide events. For example, we found that cGAS-dependent IFN-I to *Y. pseudotuberculosis* was enhanced by expression of its type 3 secretion system. Secretion systems can translocate DNA into host cells and therefore have been posited to activate cGAS, although this has not been examined in the context of *Y. pseudotuberculosis* [41, 42]. Secretion systems can also form pores on membranes, which have been linked to subsequent PAMP entry into the cytosol [43, 44]. In addition, a small percentage of pathogenic *S. aureus* (2-20%, depending on the strain and toxin expression) resides within disrupted phagosomes or freely within the cytosol of macrophages [45]. It is therefore possible that toxins produced by *S. aureus* damage phagosomes, thereby delivering CDNs into the cytosol to activate STING. Single cell studies are needed to confirm a strict link between phagosomal damage and cytosolic detection.

Bacterial-induced membrane damage, however, is unlikely to be a universal mechanism to explain CDN or DNA entry to all bacteria. Indeed, several bacteria in our panel do not possess any known toxins or membrane-penetrating secretion systems, yet they stimulated STING. Moreover, we found that non-pathogenic, laboratory *E. coli* that overproduce c-di-AMP stimulated STING independently of bacterial viability, a generally accepted prerequisite for phagosomal damage and escape. For these bacteria, other mechanisms must exist to explain CDN exodus from phagosomes and STING activation. CDN membrane transport proteins, which might function on endosomes and phagosomes, have been identified in macrophages, although it is unknown whether they function in the context of bacterial infection [38, 39, 46-50]. Moreover, pure CDN and pure DNA complexed with

membranolytic antimicrobial proteins, such as LL-37 and neutrophil elastase, exhibit increased entry into the cytosol that first requires endocytosis [51-53]. These findings suggest that antimicrobials natural to the phagosomal compartment could assist in PAMP entry into the cytosol.

We found that CDN abundance in bacteria is an important prerequisite dictating direct STING stimulation. CDNs control a variety of cellular processes in bacteria, including cell wall synthesis and DNA damage repair [37]. As under- or over-production of CDNs can have dramatic effects on bacterial activities, CDN levels are tightly regulated [37]. Notably, we bypassed CDN regulation in *E. coli*, which naturally synthesizes 3'3'-c-di-GMP, by engineering bacteria to produce non-native CDNs [33]. DacA, DncV, and cGAS synthesize 3'3'-c-di-AMP, 3'3'-cGAMP, and 2'3'-cGAMP, respectively, and *E. coli* independently expressing these enzymes potently stimulated STING independently of cGAS. Thus, CDN abundance in bacteria is sufficient for direct STING stimulation.

This work supports a new framework for how we view the role of STING in innate immunity. Rather than only sensing pathogens, we propose that STING and TLRs are common sensors of bacterial encounters. A fundamental question therefore arises for how STING ligands are delivered across phagosomal membranes. In the context of virulent pathogens, we suggest that the mechanism of CDN release from phagosomes are diverse. However, in the context of the more common encounter that occur with non-pathogens, a common mechanism of CDN transport may exist. We propose that the use of non-pathogens may be the key to unlocking the means by which STING is activated, and this means is likely coordinated around the actions of phagosomes. It has long been appreciated that phagosomes relay information about their bacterial contents to the host cell via inside-out TLR signaling [54]. We can now add a new feature to this paradigm, whereby phagosomes containing diverse bacteria also permit PAMP exodus for subsequent cytosolic PRR detection. Future studies delineating the precise rules underlying this process will likely reveal cell biological inflection points in phagosomes that control how molecules cross membranes and the immunological consequences for this crossing. This knowledge would provide a mandate to target phagosome-based inflection points as a means of immune modulation.

Materials and Methods

Antibodies and PAMPs

Antibodies against total STAT1 (#9172S), pS365-STING (#72971S), total STING (#13647), cGAS (#D3O8O), RIP2 (#4142), MAVS (#4983S), pS172-TBK1 (#D52C2), total TBK1 (#3504), pS396-IRF3 (#4947S), and total IRF3 (#4302S) were purchased from CST. The pY701-STAT1 antibody was purchased from BD (#612133). The Viperin antibody was purchased from EMD (#MABF106). The β-tubulin antibody was purchased from DSHB (#E7).

E. coli LPS (serogroup O55:B5) was purchased from Enzo (ALX-581-013-L002). 2'3'-c-di-AM(PS)2 (Rp, Rp) (#tlrl-nacda2r), lipoteichoic acid (#tlrl-pslta), Poly(I:C) (#tlrl-pic), N-glycolylated muramyl dipeptide (#tlrl-gmdp), and R848 (#tlrl-r848-5) were purchased from Invivogen. Sendai virus (SeV, Cantell Strain) supplied as allantoic fluid was sourced from Charles River Laboratory (#10100774). Calf thymus DNA (CT DNA) was purchased from Sigma (#D1501-100MG).

Cell Culture and Primary Macrophage Differentiation

Immortalized bone marrow macrophages (iBMMs), M-CSF-secreting L929 fibroblasts, and HEK293T cells were cultured at 37˚C with 5% CO_2 in DMEM (Gibco #11995-065) supplemented with 10% fetal bovine serum (FBS, Gibco #26140-079), 1x penicillin/streptomycin antibiotics (Gibco #15140-122), 1x L-glutamine (#25030-081), and 1x sodium pyruvate (#11360-070), herein referred to as complete DMEM (cDMEM). For passaging, iBMMs were lifted with 1xPBS (Gibco#10010-023) supplemented with 2.5mM EDTA (Invitrogen #15575-038) and replated with cDMEM at a dilution ratio of 1:10 on TC-treated plastic. L929 and HEK293T cells were lifted with Trypsin-EDTA (ThermoFisher #25200-114), trypsin inactivated with an equal volume of cDMEM, cells centrifuged at 400xg 5 min, and the cell pellet resuspended in cDMEM and plated on TC-treated plastic. WT and *Myd88*$^{-/-}$*Trif*$^{-/-}$ iBMMs were previously generated in our lab [55].

For primary bone marrow-derived macrophages, L929 cells were grown to confluency, incubated for 48 hrs, and M-CSF-containing supernatants were then collected and passaged through a 0.22µm filter. The femurs and tibiae of dead male and female C57BL/6 mice (6-10 weeks old, Jackson Laboratories) were cleaned, cut with scissors, and centrifuged at 800xg for 5min to pellet the bone marrow. The bone marrow pellet was then resuspended in 1xPBS supplemented with 1x antibiotic/antimycotic (ThermoFisher #15240112), passaged through a 70µm filter, and centrifuged at 400xg for 5min. The bone marrow pellet was then resuspended in

differentiation medium (*i.e.,* DMEM supplemented with 10% FBS, 1x antibiotic/antimycotic, and 30% L929 supernatant) at a concentration of $0.4x10^6$ cells/mL, plated on non-TC-treated 10cm dishes (10mL per plate), and incubated at 37˚C with 5% CO_2 (Day 0). At day 3, 5mL of differentiation medium was added. At day 6, cells were lifted with 1xPBS supplemented with 2.5mM EDTA, centrifuged at 400xg 5min, and the pellet resuspended in DMEM supplemented with 10% FBS and 5% L929 supernatant at a concentration of $0.5x10^6$ cells/mL. 1mL BMDMs were plated in each well of a 24-well TC-treated plate and allowed to adhere overnight at 37˚C with 5% CO_2. Prior to infection, BMDM supernatants were aspirated from each well and 1mL DMEM supplemented with 10% FBS and 5% L929 supernatant was added to each well and remained present throughout the experiment.

Bacterial Strains and Growth Conditions

Strains used in this study are summarized in **Supplemental Table 1**. WT strains of *L. innocua* (#33091), *L. lactis* (#19435), *L. plantarum* (#14917), *M. luteus* (#4698), *E. faecalis* (#10100), *B. subtilis* (#6633), and *N. perflava* (#14799) were purchased from ATCC. WT *S. aureus* strain SA113 (ATCC #35556) was a gift from David Underhill. WT *S. epidermidis* was a gift from Paula Watnick [56]. WT strains of *B. fragilis* and *B. thetaiotaomicron* were a gift from Dennis Kasper [57] and Andy Goodman [58], respectively. These *Bacteroides* possess modified LPS that poorly stimulates TLR4 [59, 60]. WT K12 *E. coli* is strain MG1655. *Y. pseudotuberculosis* used in this study was a gift from Igor Brodsky and is a plasmid-cured IP2666 strain that carries the mCD1 plasmid [61]; mCD1 is modified to carry all the genes necessary to build a type 3 secretion system but lacks all effector and chaperone genes [62]. Rosetta(DE3)pLysS competent *E. coli* were purchased from Novagen (#70956).

S. aureus, *S. epidermidis*, and *E. coli* (K12 and Rosetta) were cultured on Luria Broth (LB, Invitrogen #12-780-052) agar (1.5% w/v, BD #214010) at 37˚C. *L. innocua* and *E. faecalis* were cultured on Brain Heart Infusion (BHI, BD #237500) agar at 37˚C. *B. subtilis* was cultured on BHI agar at 30˚C. *L. lactis* was cultured on BHI agar at 37˚C with 5% CO_2. *L. plantarum* was cultured on lactobacilli MRS broth (BD #288130) agar at 37˚C with 5% CO_2. *M. luteus* was cultured on tryptic soy broth (TSB, BD #211825) agar at 30˚C. *Y. pseudotuberculosis* was cultured on 2xYT broth (0.5% w/v NaCl, 1.6% w/v tryptone, 1% w/v yeast extract) agar at 26˚C. *N. perflava* was cultured on Gonococcal medium base (GCB, BD #DF0289-17-3) plus Kellogg's supplements [63] at 37˚C with 5% CO_2. *B. fragilis* and *B. thetaiotaomicron* were cultured on trypticase soy-agar plates with 5% v/v sheep

blood (ThermoFisher #B21239X) at 37˚C while contained within an anaerobic chamber (BD GasPak #260683), as according to manufacturer's instructions.

Bacterial Infections

To prepare bacteria for infection, *S. aureus*, *S. epidermidis*, and *E. coli* (K-12 and Rosetta) colonies were inoculated into liquid LB and grown overnight aerobically at 37˚C. For Rosetta *E. coli*, 25µg/mL chloramphenicol (to select for pLysS) and/or 50µg/mL kanamycin (to select for pET28a(+) constructs) were used throughout growth. To induce protein expression, Rosetta *E. coli* were treated with isopropyl β-D-1-thiogalactopyranoside (IPTG) at indicated concentrations for 3 hrs just prior to infection. *L. innocua* and *E. faecalis* colonies were inoculated into liquid BHI and grown overnight aerobically at 37˚C. *L. lactis* and *L. plantarum* colonies were inoculated into liquid BHI or MRS, respectively, supplemented with 0.042% w/v $NaHCO_3$, and grown overnight aerobically at 37˚C. *B. subtilis* and *M. luteus* colonies were inoculated into liquid BHI and TSB, respectively, and grown overnight aerobically at 30˚C. *N. perflava* colonies were inoculated onto GCB agar, grown overnight at 37˚C with 5% CO_2, and stationary phase bacteria swabbed into liquid gonococcal media (1.5% w/v proteose peptone #3, 0.4% w/v K_2HPO_4, 0.1% w/v KH_2PO_4, and 0.1% w/v NaCl, pH 7.2) modified with Kellogg's supplements and 0.042% w/v $NaHCO_3$. Stationary phase bacteria in liquid cultures (*i.e.,* overnight cultures from above) were then subjected to two back dilutions (for *M. luteus*, one back dilution) to enrich for highly viable, logarithmic phase cultures that were used for infections. *Y. pseudotuberculosis* colonies were inoculated into liquid 2xYT and grown overnight aerobically at 26˚C. *Y. pseudotuberculosis* overnight cultures were subsequently back diluted and induced for expression of the type 3 secretion system as previously described [64]. Where indicated for non-inducing conditions, *Y. pseudotuberculosis* overnight cultures were back diluted into 2xYT and grown for 3 hrs aerobically at 26˚C. *B. fragilis* and *B. thetaiotaomicron* colonies were inoculated onto agar as described above for 48 hrs anaerobically prior to being swabbed into BHI liquid media for its immediate use in infections. At the time of infection, bacteria were centrifuged at 10,000xg 3 min, supernatant discarded, and pellets suspended in DMEM supplemented with 10% heat-inactivated FBS, 1x L-glutamine (#25030-081), 1x sodium pyruvate (#11360-070), herein referred to as infection DMEM (iDMEM). Bacteria suspended in iDMEM were plated to confirm multiplicity of infection (MOI).

To prepare iBMMs for infections, cultured iBMMs were centrifuged at 400xg 5 min, the pellet resuspended to a concentration of $0.5x10^6$ cells/mL in iDMEM, and 1mL cells was seeded into each well of a 24-well TC-

treated plate. Seeded iBMMs were allowed to adhere for at least 4 hrs at 37˚C with 5% CO_2. To initiate a synchronous infection, adherent iBMMs were placed on ice for 5 min, supernatants aspirated, and then cells were exposed to 1mL bacteria at the indicated MOI or 1mL PAMPs at the indicated concentration. The cells were centrifuged at 400xg 5min 4˚C to initiate bacterial contact with iBMMs. The infection was incubated for 1 hr at 37˚C with 5% CO_2 to allow for phagocytosis, after which infected supernatants were aspirated to remove non-adherent, extracellular bacteria. cDMEM containing 1x pen/strep was then added to eliminate remaining extracellular bacteria, and the infection was allowed to proceed at 37˚C with 5% CO_2 for the total indicated time.

In cases where bacteria were inactivated prior to infection, pellets containing $1x10^8$ CFU (as grown above) were resuspended in 1mL 4% paraformaldehyde (PFA) in 1x PBS and incubated for 15 min at room temperature. PFA-inactivated bacteria were then centrifuged at 10,000xg 3 min, PFA supernatants removed, and pellets washed with 1mL 1xPBS. After one more centrifugation step, the pellet of PFA-inactivated bacteria was resuspended in iDMEM and plated to confirm bacterial inactivation. For cell association experiments by flow cytometry, bacteria were labelled with 5-(and-6)-carboxyfluorescein diacetate, succinimidyl ester (CFSE) as in [65] and exposed to macrophages as above. After 2 hrs total incubation, macrophage supernatants were aspirated, cells washed once with 1mL 1xPBS, and then cells lifted with 1xPBS with 2.5mM EDTA. Cells were then centrifuged at 400xg 5min, supernatants aspirated, and cells fixed with 1% PFA in 1xPBS. Data were acquired on a LSRFortessa™ cell analyzer (BD) and analyzed using FlowJo. For experiments using bacterial conditioned supernatants, Rosetta *E. coli* and *E. coli::dacA*+ were grown as above, except with the following modification at the final back dilution step: centrifuged 2mL culture at 10,000xg 3 min, resuspended pellet in 16mL iDMEM (without phenol red) with 0.01mM IPTG, and cultured aerobically for 3 hrs 37˚C. Live bacteria were prepared as above, while the remaining cultures were then equilibrated to an equivalent OD_{600} with iDMEM, centrifuged at 4,122xg 5min, the supernatants passaged through a 0.22µm filter, and 1mL supernatants were applied to $0.5x10^6$ macrophages per well.

For SeV infection, SeV was diluted in DMEM supplemented with 1% FBS in a total volume of 100µL per well for an MOI of 0.00001. iBMMs were exposed to SeV for 1 hr at 37˚C with 5% CO_2 during which plates were gently rocked every 10 min. After 1 hr, supernatants were removed, replaced with 1mL cDMEM, and infection incubated at 37˚C with 5% CO_2 for total indicated time. All PAMPs were diluted in iDMEM to the indicated concentration for exposure to macrophages. For CT DNA, 0.9µg CT DNA was incubated with 97µL Opti-MEM

and 3μL Lipofectamine-2000 (ThermoFisher #11668019) for at least 20 min prior to infection. Supernatants from macrophages were aspirated and 900μL iDMEM added, prior to drop-wise addition of 100uL CT DNA-lipofectamine for a final concentration of 1μg/mL CT DNA per well. For cytochalasin D (cytoD, Sigma #C8273-5MG) treatment, iBMMs were treated with vehicle (DMSO) or 10μg/mL cytoD for 10 min prior to and throughout infection. For the H-151 STING inhibitor (Invivogen #inh-h151), macrophages were treated with vehicle (DMSO) or 1μg/mL H-151 for 1 hr prior to and throughout infection. For TBK1 inhibition via MRT67307 (Selleckchem #S6386), iBMMs were treated with vehicle (DMSO) or 2.5μL MRT67307 for 45min prior to and throughout infection.

Cloning and CRISPR

To generate gene knockouts in WT and *Myd88*$^{-/-}$*Trif*$^{-/-}$ iBMMs via CRISPR-Cas9, guide oligos targeting the genes of interest were designed with CRISPick (https://portals.broadinstitute.org/gppx/crispick/public) and are listed in **Supplemental Table 2**. One guide was previously published [66]. To phosphorylate and anneal guide oligos, 2μL each of 50μM sense and 50μM antisense oligos were mixed with 1X T4 ligase buffer (NEB #B0202S) and 0.5μL T4 polynucleotide kinase (NEB #M0201S) for a total 10μL reaction. The reaction mixture was incubated in a thermal cycler with the following steps: 1) 37˚C for 30 min, 2) 95˚C for 5 min, 3) 2˚C/sec decrease to 85˚C, 4) 85˚C for 1 min, and 5) 0.1˚C/sec decrease to 25˚C. Phosphorylated, annealed oligos were diluted 1:20 in molecular grade H_2O and then ligated into Esp3I-digested pLentiCRISPR V2.0 (Addgene #52961). Ligation reactions were then transformed into Top10 competent *E. coli* (ThermoFisher #C404010) and selected with 100μg/mL ampicillin to create pLentiCRISPR-ifnar1_g1, pLentiCRISPR-irf3_g1, pLentiCRISPR-tbk1_g1, pLentiCRISPR-mavs_g1, pLentiCRISPR-rip2_g1, pLentiCRISPR-sting_g1, pLentiCRISPR-cGAS_g1.

To transduce iBMMs with lentivirus, 2.5x10^6 HEK293T cells were seeded into a 10cm TC-treated dish and incubated overnight at 37˚C with 5% CO_2. HEK293T cells were then transfected with 10μg of pLentiCRISPR with the CRISPR guide of interest, 10μg of psPAX2, 2.5μg pCMV-VSVG, and Lipofectamine 2000, according to manufacturer's instructions. After an overnight incubation at 37˚C with 5% CO_2, supernatants were aspirated from transfected cells, 6mL cDMEM added, and cells incubated for 24 hrs at 37˚C with 5% CO_2. 0.5x10^6 iBMMs were plated per well of a 6-well TC plate and incubated overnight at 37˚C with 5% CO_2. 24hr viral particle-laden supernatants were harvested, centrifuged at 400xg 5 min, passaged through a 0.45μm filter, and mixed with 0.05% v/v Polybrene (Millipore TR-1003-G). iBMM supernatants were aspirated and cells exposed to the

prepared virus mixture and centrifuged at 1250xg 1 hr at 30˚C. Transduced cells were allowed to rest with added cDMEM for 24 hrs, and then cells were subjected to one more round of viral transduction. After 24hrs rest, cells were exposed to cDMEM supplemented with 10µg/mL puromycin (Gibco #A11138-03) for one week to select for transduced cells. To identify single CRISPR knockout clones, puromycin-selected cells were diluted to 1 cell per well in a 96-well TC-treated plate and allowed to propagate. Clones were confirmed as knockouts via loss of protein expression by immunoblot. In the case of IFNAR1 knockouts, clones were screened by their loss of ability to produce IP-10 to recombinant IFNβ (Biolegend #581302).

To create engineered *E. coli*, gBlocks of cyclases were designed with a C-terminal 3X-FLAG tag and codon optimized for expression in *E. coli* (see **Supplemental Table 3**). gBlocks were digested with BamHI and EcoRI and ligated into pET28a(+), which contains an IPTG-inducible lac promoter, to create pET28a(+)-*dacA*, pET28a(+)-*dncV*, and pET28a(+)-*cGAS*. Rosetta *E. coli* were then transformed with the pET28a(+) vectors and selected with 50µg/mL kanamycin to create *E. coli::dacA*+, *E. coli::dncV*+, and *E. coli::cGAS*+. To mutate DacA residues R_{208}, H_{209}, and R_{210} each to alanine, Q5 mutagenesis (NEB # E0554S) was performed using pET28a(+)-*dacA* and the forward primer 5' CGCAGCAGCTGTTGGAATCAGC 3' and reverse primer 5' GCAGCGGTACCCAGGCTTTTGCT 3' (alanine codons underlined), as per the manufacturer's instructions. The resulting plasmid, pET28a(+)-$dacA_{RHR_AAA}$ was then used to transform Rosetta *E. coli* to create *E. coli::*$dacA_{RHR_AAA}$+.

ELISA, immunoblotting, and quantitative reverse transcription polymerase chain reaction (qRT-PCR)

Macrophages exposed to bacteria and PAMPs were centrifuged at 400xg 5 min prior to analyses. Conditioned supernatants were collected, stored at -20˚C, and assayed by ELISA using IFNβ (Invivogen #luex-mifnbv2), IP-10 (R&D #DY466), and TNFα (Invitrogen #88-7324-88) kits, according to manufacturer's instructions. ELISA absorbance and luminescent readings were measured with a Tecan Spark 10M Multi-Mode Plate Reader.

Protein lysates were prepared by adding 250µL 1x sample buffer (12mM Tris-HCl pH 6.8, 0.4% w/v SDS, 5% v.v glycerol, 0.02% w/v bromophenol blue, 1% v/v β-mercaptoethanol) per well of macrophages. Protein lysates were then boiled for 5 min prior to separation via Tris-Glycine SDS-PAGE gels. Proteins were then transferred onto PVDF membranes, which were subsequently blocked with 5% BSA in 1xTBS with 0.1% Tween-20 (TBS-T). Antibodies were diluted in 1% BSA TBS-T, according the manufacturer's recommendations (except, anti-

pS365-STING, which was diluted 1:100). Blots were incubated with primary antibodies overnight at 4˚C, and blots were incubated with secondary antibodies for 1 hr at RT. Blots were washed 5x with TBS-T before and after the secondary antibody incubation. Membranes were incubated with SuperSignal West Pico or Femto Chemiluminescent substrate (ThermoFisher), and images of blots were acquired on a ChemiDoc XRS+ System (BioRad).

For RNA, macrophages were lysed with 300µL lysis buffer with 1% v/v β-mercaptoethanol (Themo #12183025) and passaged through a QIAshredder homogenizer column (Qiagen #79656). Total RNA was isolated (Themo #12183025) and treated with DNaseI (ThermoFisher #EN0521), according to the manufacturer's instructions. 30 ng of RNA was used per well (of a 384-well plate format) for detection. Reverse transcription and PCR was performed in a 384-well format on a CFX384 Touch Real-Time PCR detection system (BioRad) using the Taqman RNA-to-CT 1-Step kit (ThermoFisher #4392938), according to manufacturer's instructions. Genes were detected by Taqman probes (Mm01277042_m1 for *tbp*; Mm00439552_s1 for *ifnb1*; Mm00491265_m1for *rsad2*; and Mm99999068_m1 for *tnf*).

Statistics

All values, unless otherwise indicated, represent the mean ± the standard error of the mean (SEM) of at least 3 independent replicates. A two tailed student's *t*-test was performed, unless otherwise noted, to determine significance, which was defined as a *p*-value less than 0.05.

Acknowledgements

We would like to thank Igor Brodsky, David Underhill, Paula Watnick, Dennis Kasper, and Andy Goodman for bacteria used in this study. We would also like to thank all members for the Kagan Laboratory for their helpful discussions and support. S.A.R. was supported by postdoctoral fellowship from the Jane Coffin Childs Memorial Fund for Medical Research. This work was supported by NIH grants AI133524, AI093589, AI116550, and P30DK34854 to J.C.K.

References

1. Pandey S, Kawai T, Akira S. Microbial sensing by Toll-like receptors and intracellular nucleic acid sensors. Cold Spring Harb Perspect Biol. 2014;7(1):a016246. Epub 2014/10/11. doi: 10.1101/cshperspect.a016246. PubMed PMID: 25301932; PubMed Central PMCID: PMCPMC4292165.

2. Decout A, Katz JD, Venkatraman S, Ablasser A. The cGAS-STING pathway as a therapeutic target in inflammatory diseases. Nat Rev Immunol. 2021. Epub 2021/04/10. doi: 10.1038/s41577-021-00524-z. PubMed PMID: 33833439; PubMed Central PMCID: PMCPMC8029610.

3. Zaver SA, Woodward JJ. Cyclic dinucleotides at the forefront of innate immunity. Curr Opin Cell Biol. 2020;63:49-56. Epub 2020/01/21. doi: 10.1016/j.ceb.2019.12.004. PubMed PMID: 31958669; PubMed Central PMCID: PMCPMC7247925.

4. Fitzgerald KA, Kagan JC. Toll-like Receptors and the Control of Immunity. Cell. 2020;180(6):1044-66. Epub 2020/03/14. doi: 10.1016/j.cell.2020.02.041. PubMed PMID: 32164908.

5. Stocks CJ, Schembri MA, Sweet MJ, Kapetanovic R. For when bacterial infections persist: Toll-like receptor-inducible direct antimicrobial pathways in macrophages. J Leukoc Biol. 2018;103(1):35-51. Epub 2018/01/19. doi: 10.1002/JLB.4RI0917-358R. PubMed PMID: 29345056.

6. Evavold CL, Kagan JC. How Inflammasomes Inform Adaptive Immunity. J Mol Biol. 2018;430(2):217-37. Epub 2017/10/11. doi: 10.1016/j.jmb.2017.09.019. PubMed PMID: 28987733; PubMed Central PMCID: PMCPMC5766381.

7. Brubaker SW, Bonham KS, Zanoni I, Kagan JC. Innate immune pattern recognition: a cell biological perspective. Annu Rev Immunol. 2015;33:257-90. Epub 2015/01/13. doi: 10.1146/annurev-immunol-032414-112240. PubMed PMID: 25581309; PubMed Central PMCID: PMCPMC5146691.

8. Evavold CL, Kagan JC. Inflammasomes: Threat-Assessment Organelles of the Innate Immune System. Immunity. 2019;51(4):609-24. Epub 2019/09/02. doi: 10.1016/j.immuni.2019.08.005. PubMed PMID: 31473100; PubMed Central PMCID: PMCPMC6801093.

9. Abdullah Z, Knolle PA. Scaling of immune responses against intracellular bacterial infection. EMBO J. 2014;33(20):2283-94. Epub 2014/09/17. doi: 10.15252/embj.201489055. PubMed PMID: 25225613; PubMed Central PMCID: PMCPMC4253520.

10. Ragland SA, Kagan JC. Cytosolic detection of phagosomal bacteria-Mechanisms underlying PAMP exodus from the phagosome into the cytosol. Mol Microbiol. 2021;116(6):1420-32. Epub 2021/11/06. doi: 10.1111/mmi.14841. PubMed PMID: 34738270; PubMed Central PMCID: PMCPMC8688326.

11. Ruangkiattikul N, Nerlich A, Abdissa K, Lienenklaus S, Suwandi A, Janze N, et al. cGAS-STING-TBK1-IRF3/7 induced interferon-beta contributes to the clearing of non tuberculous mycobacterial infection in mice. Virulence. 2017;8(7):1303-15. Epub 2017/04/20. doi: 10.1080/21505594.2017.1321191. PubMed PMID: 28422568; PubMed Central PMCID: PMCPMC5711412.

12. Case CL, Kohler LJ, Lima JB, Strowig T, de Zoete MR, Flavell RA, et al. Caspase-11 stimulates rapid flagellin-independent pyroptosis in response to Legionella pneumophila. Proc Natl Acad Sci U S A. 2013;110(5):1851-6. Epub 2013/01/12. doi: 10.1073/pnas.1211521110. PubMed PMID: 23307811; PubMed Central PMCID: PMCPMC3562791.

13. Balakrishnan A, Karki R, Berwin B, Yamamoto M, Kanneganti TD. Guanylate binding proteins facilitate caspase-11-dependent pyroptosis in response to type 3 secretion system-negative Pseudomonas aeruginosa. Cell Death Discov. 2018;4:3. Epub 2018/08/01. doi: 10.1038/s41420-018-0068-z. PubMed PMID: 30062052; PubMed Central PMCID: PMCPMC6060091.

14. Moretti J, Roy S, Bozec D, Martinez J, Chapman JR, Ueberheide B, et al. STING Senses Microbial Viability to Orchestrate Stress-Mediated Autophagy of the Endoplasmic Reticulum. Cell. 2017;171(4):809-23 e13. Epub 2017/10/24. doi: 10.1016/j.cell.2017.09.034. PubMed PMID: 29056340; PubMed Central PMCID: PMCPMC5811766.

15. Cheung GYC, Bae JS, Otto M. Pathogenicity and virulence of Staphylococcus aureus. Virulence. 2021;12(1):547-69. Epub 2021/02/02. doi: 10.1080/21505594.2021.1878688. PubMed PMID: 33522395; PubMed Central PMCID: PMCPMC7872022.

16. Dib JR, Liebl W, Wagenknecht M, Farias ME, Meinhardt F. Extrachromosomal genetic elements in Micrococcus. Appl Microbiol Biotechnol. 2013;97(1):63-75. Epub 2012/11/10. doi: 10.1007/s00253-012-4539-5. PubMed PMID: 23138713.

17. Galindo CL, Rosenzweig JA, Kirtley ML, Chopra AK. Pathogenesis of Y. enterocolitica and Y. pseudotuberculosis in Human Yersiniosis. J Pathog. 2011;2011:182051. Epub 2011/01/01. doi: 10.4061/2011/182051. PubMed PMID: 22567322; PubMed Central PMCID: PMCPMC3335670.

18. Fiore E, Van Tyne D, Gilmore MS. Pathogenicity of Enterococci. Microbiol Spectr. 2019;7(4). Epub 2019/07/13. doi: 10.1128/microbiolspec.GPP3-0053-2018. PubMed PMID: 31298205; PubMed Central PMCID: PMCPMC6629438.

19. Becker K, Heilmann C, Peters G. Coagulase-negative staphylococci. Clin Microbiol Rev. 2014;27(4):870-926. Epub 2014/10/04. doi: 10.1128/CMR.00109-13. PubMed PMID: 25278577; PubMed Central PMCID: PMCPMC4187637.

20. Milillo SR, Friedly EC, Saldivar JC, Muthaiyan A, O'Bryan C, Crandall PG, et al. A review of the ecology, genomics, and stress response of Listeria innocua and Listeria monocytogenes. Crit Rev Food Sci Nutr. 2012;52(8):712-25. Epub 2012/05/18. doi: 10.1080/10408398.2010.507909. PubMed PMID: 22591342.

21. Song AA, In LLA, Lim SHE, Rahim RA. A review on Lactococcus lactis: from food to factory. Microb Cell Fact. 2017;16(1):55. Epub 2017/04/06. doi: 10.1186/s12934-017-0669-x. PubMed PMID: 28376880; PubMed Central PMCID: PMCPMC5379754.

22. Behera SS, Ray RC, Zdolec N. Lactobacillus plantarum with Functional Properties: An Approach to Increase Safety and Shelf-Life of Fermented Foods. Biomed Res Int. 2018;2018:9361614. Epub 2018/07/13. doi: 10.1155/2018/9361614. PubMed PMID: 29998137; PubMed Central PMCID: PMCPMC5994577.

23. Earl AM, Losick R, Kolter R. Ecology and genomics of Bacillus subtilis. Trends Microbiol. 2008;16(6):269-75. Epub 2008/05/10. doi: 10.1016/j.tim.2008.03.004. PubMed PMID: 18467096; PubMed Central PMCID: PMCPMC2819312.

24. Dougan G, Haque A, Pickard D, Frankel G, O'Goara P, Wain J. The Escherichia coli gene pool. Curr Opin Microbiol. 2001;4(1):90-4. Epub 2001/02/15. doi: 10.1016/s1369-5274(00)00170-3. PubMed PMID: 11173040.

25. Johnson AP. The pathogenic potential of commensal species of Neisseria. J Clin Pathol. 1983;36(2):213-23. Epub 1983/02/01. doi: 10.1136/jcp.36.2.213. PubMed PMID: 6338050; PubMed Central PMCID: PMCPMC498155.

26. Wexler AG, Goodman AL. An insider's perspective: Bacteroides as a window into the microbiome. Nat Microbiol. 2017;2:17026. Epub 2017/04/26. doi: 10.1038/nmicrobiol.2017.26. PubMed PMID: 28440278; PubMed Central PMCID: PMCPMC5679392.

27. McNab F, Mayer-Barber K, Sher A, Wack A, O'Garra A. Type I interferons in infectious disease. Nat Rev Immunol. 2015;15(2):87-103. Epub 2015/01/24. doi: 10.1038/nri3787. PubMed PMID: 25614319; PubMed Central PMCID: PMCPMC7162685.

28. Der SD, Zhou A, Williams BR, Silverman RH. Identification of genes differentially regulated by interferon alpha, beta, or gamma using oligonucleotide arrays. Proc Natl Acad Sci U S A. 1998;95(26):15623-8. Epub 1998/12/23. doi: 10.1073/pnas.95.26.15623. PubMed PMID: 9861020; PubMed Central PMCID: PMCPMC28094.

29. Auerbuch V, Golenbock DT, Isberg RR. Innate immune recognition of Yersinia pseudotuberculosis type III secretion. PLoS Pathog. 2009;5(12):e1000686. Epub 2009/12/10. doi: 10.1371/journal.ppat.1000686. PubMed PMID: 19997504; PubMed Central PMCID: PMCPMC2779593.

30. Pandey AK, Yang Y, Jiang Z, Fortune SM, Coulombe F, Behr MA, et al. NOD2, RIP2 and IRF5 play a critical role in the type I interferon response to Mycobacterium tuberculosis. PLoS Pathog. 2009;5(7):e1000500. doi: 10.1371/journal.ppat.1000500. PubMed PMID: 19578435; PubMed Central PMCID: PMCPMC2698121.

31. Haag SM, Gulen MF, Reymond L, Gibelin A, Abrami L, Decout A, et al. Targeting STING with covalent small-molecule inhibitors. Nature. 2018;559(7713):269-73. Epub 2018/07/06. doi: 10.1038/s41586-018-0287-8. PubMed PMID: 29973723.

32. Kundra S, Lam LN, Kajfasz JK, Casella LG, Andersen MJ, Abranches J, et al. c-di-AMP Is Essential for the Virulence of Enterococcus faecalis. Infect Immun. 2021;89(11):e0036521. Epub 2021/08/24. doi: 10.1128/IAI.00365-21. PubMed PMID: 34424750; PubMed Central PMCID: PMCPMC8519298.

33. Simm R, Morr M, Kader A, Nimtz M, Romling U. GGDEF and EAL domains inversely regulate cyclic di-GMP levels and transition from sessility to motility. Mol Microbiol. 2004;53(4):1123-34. Epub 2004/08/13. doi: 10.1111/j.1365-2958.2004.04206.x. PubMed PMID: 15306016.

34. Pham HT, Nhiep NTH, Vu TNM, Huynh TN, Zhu Y, Huynh ALD, et al. Enhanced uptake of potassium or glycine betaine or export of cyclic-di-AMP restores osmoresistance in a high cyclic-di-AMP Lactococcus lactis mutant. PLoS Genet. 2018;14(8):e1007574. Epub 2018/08/04. doi: 10.1371/journal.pgen.1007574. PubMed PMID: 30074984; PubMed Central PMCID: PMCPMC6108528.

35. Corrigan RM, Abbott JC, Burhenne H, Kaever V, Grundling A. c-di-AMP is a new second messenger in Staphylococcus aureus with a role in controlling cell size and envelope stress. PLoS Pathog. 2011;7(9):e1002217. Epub 2011/09/13. doi: 10.1371/journal.ppat.1002217. PubMed PMID: 21909268; PubMed Central PMCID: PMCPMC3164647.

36. Zhu Y, Pham TH, Nhiep TH, Vu NM, Marcellin E, Chakrabortti A, et al. Cyclic-di-AMP synthesis by the diadenylate cyclase CdaA is modulated by the peptidoglycan biosynthesis enzyme GlmM in Lactococcus lactis. Mol Microbiol. 2016;99(6):1015-27. Epub 2015/11/21. doi: 10.1111/mmi.13281. PubMed PMID: 26585449.

37. Krasteva PV, Sondermann H. Versatile modes of cellular regulation via cyclic dinucleotides. Nat Chem Biol. 2017;13(4):350-9. Epub 2017/03/23. doi: 10.1038/nchembio.2337. PubMed PMID: 28328921; PubMed Central PMCID: PMCPMC5773344.

38. Luteijn RD, Zaver SA, Gowen BG, Wyman SK, Garelis NE, Onia L, et al. SLC19A1 transports immunoreactive cyclic dinucleotides. Nature. 2019;573(7774):434-8. Epub 2019/09/13. doi: 10.1038/s41586-019-1553-0. PubMed PMID: 31511694; PubMed Central PMCID: PMCPMC6785039.

39. Ritchie C, Cordova AF, Hess GT, Bassik MC, Li L. SLC19A1 Is an Importer of the Immunotransmitter cGAMP. Mol Cell. 2019;75(2):372-81 e5. Epub 2019/05/28. doi: 10.1016/j.molcel.2019.05.006. PubMed PMID: 31126740; PubMed Central PMCID: PMCPMC6711396.

40. Bai Y, Yang J, Zhou X, Ding X, Eisele LE, Bai G. Mycobacterium tuberculosis Rv3586 (DacA) is a diadenylate cyclase that converts ATP or ADP into c-di-AMP. PLoS One. 2012;7(4):e35206. Epub 2012/04/25. doi: 10.1371/journal.pone.0035206. PubMed PMID: 22529992; PubMed Central PMCID: PMCPMC3328451.

41. Guzman-Herrador DL, Steiner S, Alperi A, Gonzalez-Prieto C, Roy CR, Llosa M. DNA Delivery and Genomic Integration into Mammalian Target Cells through Type IV A and B Secretion Systems of Human Pathogens. Front Microbiol. 2017;8:1503. Epub 2017/09/08. doi: 10.3389/fmicb.2017.01503. PubMed PMID: 28878740; PubMed Central PMCID: PMCPMC5572225.

42. Damke PP, Wood CR, Shaffer CL. Helicobacter pylori provokes STING immunosurveillance via trans-kingdom conjugation. bioRxiv. 2022:2022.06.29.498044. doi: 10.1101/2022.06.29.498044.

43. Casson CN, Copenhaver AM, Zwack EE, Nguyen HT, Strowig T, Javdan B, et al. Caspase-11 activation in response to bacterial secretion systems that access the host cytosol. PLoS Pathog.

2013;9(6):e1003400. Epub 2013/06/14. doi: 10.1371/journal.ppat.1003400. PubMed PMID: 23762026; PubMed Central PMCID: PMCPMC3675167.

44. Feeley EM, Pilla-Moffett DM, Zwack EE, Piro AS, Finethy R, Kolb JP, et al. Galectin-3 directs antimicrobial guanylate binding proteins to vacuoles furnished with bacterial secretion systems. Proc Natl Acad Sci U S A. 2017;114(9):E1698-E706. Epub 2017/02/15. doi: 10.1073/pnas.1615771114. PubMed PMID: 28193861; PubMed Central PMCID: PMCPMC5338555.

45. Grosz M, Kolter J, Paprotka K, Winkler AC, Schafer D, Chatterjee SS, et al. Cytoplasmic replication of Staphylococcus aureus upon phagosomal escape triggered by phenol-soluble modulin alpha. Cell Microbiol. 2014;16(4):451-65. Epub 2013/10/30. doi: 10.1111/cmi.12233. PubMed PMID: 24164701; PubMed Central PMCID: PMCPMC3969633.

46. Cordova AF, Ritchie C, Bohnert V, Li L. Human SLC46A2 Is the Dominant cGAMP Importer in Extracellular cGAMP-Sensing Macrophages and Monocytes. ACS Cent Sci. 2021;7(6):1073-88. Epub 2021/07/09. doi: 10.1021/acscentsci.1c00440. PubMed PMID: 34235268; PubMed Central PMCID: PMCPMC8228594.

47. Lahey LJ, Mardjuki RE, Wen X, Hess GT, Ritchie C, Carozza JA, et al. LRRC8A:C/E Heteromeric Channels Are Ubiquitous Transporters of cGAMP. Mol Cell. 2020;80(4):578-91 e5. Epub 2020/11/11. doi: 10.1016/j.molcel.2020.10.021. PubMed PMID: 33171122.

48. Chen X, Wang L, Cao L, Li T, Li Z, Sun Y, et al. Regulation of Anion Channel LRRC8 Volume-Regulated Anion Channels in Transport of 2'3'-Cyclic GMP-AMP and Cisplatin under Steady State and Inflammation. J Immunol. 2021;206(9):2061-74. Epub 2021/04/09. doi: 10.4049/jimmunol.2000989. PubMed PMID: 33827893.

49. Zhou C, Chen X, Planells-Cases R, Chu J, Wang L, Cao L, et al. Transfer of cGAMP into Bystander Cells via LRRC8 Volume-Regulated Anion Channels Augments STING-Mediated Interferon Responses and Anti-viral Immunity. Immunity. 2020;52(5):767-81 e6. Epub 2020/04/12. doi: 10.1016/j.immuni.2020.03.016. PubMed PMID: 32277911.

50. Zhou Y, Fei M, Zhang G, Liang WC, Lin W, Wu Y, et al. Blockade of the Phagocytic Receptor MerTK on Tumor-Associated Macrophages Enhances P2X7R-Dependent STING Activation by Tumor-Derived

cGAMP. Immunity. 2020;52(2):357-73 e9. Epub 2020/02/13. doi: 10.1016/j.immuni.2020.01.014. PubMed PMID: 32049051.

51. Apel F, Andreeva L, Knackstedt LS, Streeck R, Frese CK, Goosmann C, et al. The cytosolic DNA sensor cGAS recognizes neutrophil extracellular traps. Sci Signal. 2021;14(673). Epub 2021/03/11. doi: 10.1126/scisignal.aax7942. PubMed PMID: 33688080.

52. Chamilos G, Gregorio J, Meller S, Lande R, Kontoyiannis DP, Modlin RL, et al. Cytosolic sensing of extracellular self-DNA transported into monocytes by the antimicrobial peptide LL37. Blood. 2012;120(18):3699-707. Epub 2012/08/29. doi: 10.1182/blood-2012-01-401364. PubMed PMID: 22927244; PubMed Central PMCID: PMCPMC3488884.

53. Wei X, Zhang L, Yang Y, Hou Y, Xu Y, Wang Z, et al. LL-37 transports immunoreactive cGAMP to activate STING signaling and enhance interferon-mediated host antiviral immunity. Cell Rep. 2022;39(9):110880. Epub 2022/06/02. doi: 10.1016/j.celrep.2022.110880. PubMed PMID: 35649354.

54. Kagan JC, Iwasaki A. Phagosome as the organelle linking innate and adaptive immunity. Traffic. 2012;13(8):1053-61. Epub 2012/05/15. doi: 10.1111/j.1600-0854.2012.01377.x. PubMed PMID: 22577865; PubMed Central PMCID: PMCPMC3658133.

55. Zanoni I, Ostuni R, Marek LR, Barresi S, Barbalat R, Barton GM, et al. CD14 controls the LPS-induced endocytosis of Toll-like receptor 4. Cell. 2011;147(4):868-80. Epub 2011/11/15. doi: 10.1016/j.cell.2011.09.051. PubMed PMID: 22078883; PubMed Central PMCID: PMCPMC3217211.

56. Marek LR, Kagan JC. Phosphoinositide binding by the Toll adaptor dMyD88 controls antibacterial responses in Drosophila. Immunity. 2012;36(4):612-22. Epub 2012/04/03. doi: 10.1016/j.immuni.2012.01.019. PubMed PMID: 22464168; PubMed Central PMCID: PMCPMC3354765.

57. An D, Oh SF, Olszak T, Neves JF, Avci FY, Erturk-Hasdemir D, et al. Sphingolipids from a symbiotic microbe regulate homeostasis of host intestinal natural killer T cells. Cell. 2014;156(1-2):123-33. Epub 2014/01/21. doi: 10.1016/j.cell.2013.11.042. PubMed PMID: 24439373; PubMed Central PMCID: PMCPMC3909465.

58. Cullen TW, Schofield WB, Barry NA, Putnam EE, Rundell EA, Trent MS, et al. Gut microbiota. Antimicrobial peptide resistance mediates resilience of prominent gut commensals during inflammation.

Science. 2015;347(6218):170-5. Epub 2015/01/13. doi: 10.1126/science.1260580. PubMed PMID: 25574022; PubMed Central PMCID: PMCPMC4388331.

59. Xu J, Bjursell MK, Himrod J, Deng S, Carmichael LK, Chiang HC, et al. A genomic view of the human-Bacteroides thetaiotaomicron symbiosis. Science. 2003;299(5615):2074-6. Epub 2003/03/29. doi: 10.1126/science.1080029. PubMed PMID: 12663928.

60. Tan Y, Zanoni I, Cullen TW, Goodman AL, Kagan JC. Mechanisms of Toll-like Receptor 4 Endocytosis Reveal a Common Immune-Evasion Strategy Used by Pathogenic and Commensal Bacteria. Immunity. 2015;43(5):909-22. Epub 2015/11/08. doi: 10.1016/j.immuni.2015.10.008. PubMed PMID: 26546281; PubMed Central PMCID: PMCPMC4685471.

61. Brodsky IE, Palm NW, Sadanand S, Ryndak MB, Sutterwala FS, Flavell RA, et al. A Yersinia effector protein promotes virulence by preventing inflammasome recognition of the type III secretion system. Cell Host Microbe. 2010;7(5):376-87. Epub 2010/05/19. doi: 10.1016/j.chom.2010.04.009. PubMed PMID: 20478539; PubMed Central PMCID: PMCPMC2883865.

62. Bartra SS, Jackson MW, Ross JA, Plano GV. Calcium-regulated type III secretion of Yop proteins by an Escherichia coli hha mutant carrying a Yersinia pestis pCD1 virulence plasmid. Infect Immun. 2006;74(2):1381-6. Epub 2006/01/24. doi: 10.1128/IAI.74.2.1381-1386.2006. PubMed PMID: 16428789; PubMed Central PMCID: PMCPMC1360333.

63. Kellogg DS, Jr., Peacock WL, Jr., Deacon WE, Brown L, Pirkle DI. Neisseria Gonorrhoeae. I. Virulence Genetically Linked to Clonal Variation. J Bacteriol. 1963;85:1274-9. PubMed PMID: 14047217; PubMed Central PMCID: PMCPMC278328.

64. Brodsky IE, Medzhitov R. Reduced secretion of YopJ by Yersinia limits in vivo cell death but enhances bacterial virulence. PLoS Pathog. 2008;4(5):e1000067. Epub 2008/05/17. doi: 10.1371/journal.ppat.1000067. PubMed PMID: 18483548; PubMed Central PMCID: PMCPMC2361194.

65. Ragland SA, Humbert MV, Christodoulides M, Criss AK. Neisseria gonorrhoeae employs two protein inhibitors to evade killing by human lysozyme. PLoS Pathog. 2018;14(7):e1007080. doi: 10.1371/journal.ppat.1007080. PubMed PMID: 29975775.

66. Ding Q, Gaska JM, Douam F, Wei L, Kim D, Balev M, et al. Species-specific disruption of STING-dependent antiviral cellular defenses by the Zika virus NS2B3 protease. Proc Natl Acad Sci U S A.

2018;115(27):E6310-E8. Epub 2018/06/20. doi: 10.1073/pnas.1803406115. PubMed PMID: 29915078; PubMed Central PMCID: PMCPMC6142274.

Supplemental Tables

Supplemental Table 1. Bacterial Strains used in this study.

Species (Abbreviation)	Strain Designation	Source	Pathogen?
S. aureus (SA)	Strain SA113	ATCC #35556; Gifted by David Underhill	Opportunistic pathogen
S. epidermidis (SE)	-	Gifted by Paula Watnick	Non-pathogen
L. innocua (LI)	SLCC 3423	ATCC #33091	Non-pathogen
L. lactis (LL)	NCTC 6681	ATCC #19435	Non-pathogen
L. plantarum (LP)	LP 39	ATCC #14917	Non-pathogen
M. luteus (ML)	ATCC 15307	ATCC #4698	Non-pathogen
E. faecalis (EF)	P-60	ATCC #10100	Opportunistic pathogen
B. subtilis (BS)	NRS 231	ATCC #6633	Non-pathogen
E. coli (EC)	MG1655 (K-12)	-	Non-pathogen
N. perflava (NP)	28	ATCC #14799	Non-pathogen
Y. pseudotuberculosis (YP)	Plasmid-cured IP2666 with mCD1 plasmid	Gifted by Igor Brodsky	Pathogen
B. fragilis (BF)	-	Gifted by Dennis Kasper	Non-pathogen
B. thetaiotaomicron (BT)	-	Gifted by Andy Goodman	Non-pathogen

Supplemental Table 2. Guide Oligos used for cloning into pLentiCRISPR V. 2.0. In red are overhangs corresponding to Esp3I restriction digestion. In blue and underlined is an extra G that helps with guide expression efficiency.

Target Gene	Target Sequence	Sense Oligo	Antisense Oligo	Resulting Plasmid	Reference
Ifnar1 NCBI #15975	CTTCTAAACGTACTTCTGGG	5'CACCGCTTCTAAACGTACTTCTGGG3'	5'AAACCCCAGAAGTACGTTTAGAAGC3'	pLentiCRISPR-ifnar1_g1	This study
Irf3 NCBI #54131	CCAGTGGTGCCTACACCCCG	5'CACCGCCAGTGGTGCCTACACCCCG3'	5'AAACCGGGGTGTAGGCACCACTGC3'	pLentiCRISPR-irf3_g1	This study
Tbk1 NCBI #56480	CAACATCATGCGCGTCATAG	5'CACCGCAACATCATGCGCGTCATAG3'	5'AAACCTATGACGCGCATGATGTTGC3'	pLentiCRISPR-tbk1_g1	This study
Mavs NCBI #228607	GTGACCTGGCGCAAATGCAG	5'CACCGGTGACCTGGCGCAAATGCAG3'	5'AAACCTGCATTTGCGCCAGGTCACC3'	pLentiCRISPR-mavs_g1	This study
Rip2 NCBI #192656	TAGGTCATGATGAAGCAGAG	5'CACCGTAGGTCATGATGAAGCAGAG3'	5'AAACCTCTGCTTCATCATGACCTAC3'	pLentiCRISPR-rip2_g1	This study
Sting1 NCBI #72512	TACTTGCGGTTGATCTTACC	5'CACCGTACTTGCGGTTGATCTTACC3'	5'AAACGGTAAGATCAACCGCAAGTAC3'	pLentiCRISPR-sting_g1	Ding *et al.*, 2018
cGAS NCBI #214763	GAAACGCAAAGATATCTCGG	5'CACCGGAAACGCAAAGATATCTCGG3'	5'AAACCCGAGATATCTTTGCGTTTCC3'	pLentiCRISPR-cGAS_g1	This study

Supplemental Table 3. gBlock design used for cloning into pET28a(+) in this study. In blue and pink text are the BamHI and EcoRI sites, respectively. Stop codon is in red text. C-terminal 3xFLAG sequence and linker is underlined.

Organism and Gene	gBlock Sequence	Resulting Plasmid
S. aureus dacA (strain Newman)	ATCCAGGATCCGATTTCTCTAACTTCTTCCAAAATTTATCCACGCTTAAAATCGTGACCTCGATTT TGGATCTGCTGATTGTATGGTATGTGTTGTATTTGTTGATCACTGTTTTTAAGGGCACCAAAGCA ATTCAACTTCTGAAGGGAATCCTTGTCATTGTGATCGGCCAACAGATCTCGATGATTTTGAATCT TACTGCTACGTCTAAACTTTTTGATATCGTGATTCAGTGGGGCGTGCTGGCGCTGATTGTTATCT TCCAGCCCGAAATTCGCCGCGCATTAGAGCAACTTGGTCGCGGCTCTTTTTTGAAACGCTATAC GAGCAATACCTACAGCAAGGACGAGGAAAAATTAATCCAATCAGTTTCAAAAGCTGTGCAATAC ATGGCCAAACGTCGTATTGGTGCGTTGATTGTGTTCGAAAAAGAAACGGGTCTTCAAGACTACA TCGAAACTGGTATTGCAATGGACAGTAACATTTCTCAAGAACTGCTTATTAACGTCTTCATCCCA AACACCCCTTTGCATGACGGCGCAATGATTATTCAAGGTACCAAGATTGCCGCCGCGGCCAGC TATCTGCCCTTATCGGATAGTCCGAAGATTAGCAAAAGCCTGGGTACCCGTCACCGCGCAGCT GTTGGAATCAGCGAGGTGTCGGATGCTTTTACGGTGATCGTGAGCGAAGAAACAGGAGATATC TCGGTTACATTCGATGGGAAACTTCGTCGTGACATCTCGAATGAAATTTTTGAGGAATTACTTGC AGAGCACTGGTTCGGCACGCGTTTCCAAAAGAAAGGCGTAAAAGACTACAAGGATCATGATGG TGATTACAAGGATCATGACATTGACTATAAAGATGACGACGATAAAGACTACAAGGACGATGAC GATAAAGATTATAAGGATGACGACGATAAGTGAGAATTCATCG	pET28a(+)-*dacA*
V. cholerae dncV (strain O1 El Tor N16961)	ATCCAGGATCCAGAATGACTTGGAATTTCCACCAATATTACACCAACCGCAACGACGGTCTTAT GGGGAAGCTGGTTTTAACCGATGAAGAAAAAAACAACCTGAAGGCGCTTCGTAAGATTATCCGC TTGCGCACACGCGATGTTTTTGAAGAAGCCAAAGGAATCGCGAAAGCAGTGAAGAAAAGTGCTT TGACATTCGAGATCATTCAAGAAAAAGTGTCGACCACTCAGATTAAACATCTGTCCGATTCCGAG CAACGTGAAGTCGCAAAATTAATCTATGAGATGGACGATGATGCTCGCGACGAGTTTTTGGGGT TAACCCCACGCTTTTGGACGCAAGGTTCATTTCAATACGATACCTTGAACCGTCCCTTTCAACCG GGTCAAGAGATGGATATTGATGACGGCACATATATGCCTATGCCCATTTTCGAATCCGAGCCAA AAATCGGGCATTCCCTTTTAATCCTTTTGGTCGATGCCTCTTTGAAAAGCTTGGTGGCCGAGAA CCATGGATGGAAATTTGAGGCAAAACAAACGTGTGGTCGTATTAAAATCGAAGCCGAGAAAACC CATATCGACGTGCCCATGTATGCCATCCCCAAGGACGAATTTCAGAAGAAGCAGATCGCTTTGG AGGCCAACCGTTCCTTCGTGAAGGGCGCAATTTTCGAAAGCTACGTAGCTGACTCTATTACAGA CGACAGCGAAACATACGAGTTGGATTCCGAAAACGTCAACTTAGCCCTGCGCGAGGGCGACCG TAAATGGATTAATTCAGATCCCAAGATCGTAGAGGACTGGTTCAACGACAGCTGTATTCGTATC GGGAAACACTTGCGTAAAGTTTGTCGCTTTATGAAGGCGTGGCGTGATGCTCAGTGGGACGTT GGCGGTCCTTCCTCGATCAGCTTAATGGCTGCGACCGTCAACATTTTGGATTCCGTAGCACACG ATGCATCAGACCTTGGTGAAACGATGAAAATTATTGCCAAGCACCTGCCCTCGGAGTTTGCCCG CGGTGTGGAGAGTCCGGACAGTACTGACGAGAAACCTTTGTTCCCGCCGTCATATAAGCACGG GCCTCGTGAAATGGACATTATGTCAAAGCTGGAACGTCTTCCGGAAATCTTAAGCAGTGCTGAA TCCGCAGACTCTAAGTCCGAAGCACTTAAAAAGATCAATATGGCGTTCGGCAATCGCGTTACCA ATTCCGAGCTTATCGTCTTGGCCAAAGCCCTGCCGGCCTTTGCCCAGGAGCCAAGTTCGGCTT CTAAGCCAGAGAAAATTTCGTCAACGATGGTTAGTGGCGATTACAAGGACCATGATGGTGATTA CAAAGACCATGATATCGACTATAAGGACGACGATGATAAAGATTATAAGGACGACGACGACAAG GACTACAAGGATGATGACGATAAGTGAGAATTCATCG	pET28a(+)-*dncV*
M. musculus cGAS	ATCCAGGATCCGAAGACCCCCGTCGCCGTACGACGGCACCACGCGCCAAAAAACCGAGCGCC AAGCGTGCTCCAACGCAGCCTAGTCGTACTCGTGCACATGCGGAATCCTGCGGCCCCCAACGC GGGGCGCGCTCGCGTCGCGCTGAGCGTGACGGGGATACTACCGAAAAACCACGCGCACCTGG CCCTCGCGTACACCCGGCCCGTGCAACAGAATTAACGAAAGACGCTCAACCTTCAGCTATGGA CGCGGCTGGAGCGACAGCTCGTCCAGCTGTACGCGTTCCCCAACAACAAGCGATCCTTGACCC GGAGCTTCCTGCTGTTCGCGAGCCACAGCCCCCAGCAGATCCTGAGGCGCGTAAAGTCGTGC GTGGGCCTTCGCACCGCCGCGGCGCTCGCTCTACCGGACAACCGCGTGCCCCGCGCGGGAG CCGCAAGGAGCCAGACAAGCTGAAAAAAGTTTTAGATAAGTTACGTTTAAAACGTAAAGACATC AGTGAGGCGGCAGAAACTGTTAATAAGGTCGTAGAGCGCCTTTTACGTCGTATGCAAAAACGTG AGTCTGAGTTCAAGGGTGTGGAGCAGCTGAACACAGGTTCATACTACGAGCACGTGAAGATCT CTGCTCCAAATGAGTTTGACGTAATGTTCAAGTTAGAGGTGCCTCGTATCGAACTGCAGGAGTA CTATGAGACAGGAGCCTTCTACCTTGTCAAGTTCAAGCGTATCCCCCGCGGTAACCCTTTGTCT CACTTCTTGGAAGGTGAAGTGCTTAGTGCTACGAAGATGTTGTCCAAGTTCCGCAAGATTATTAA GGAAGAGGTGAAAAGAGATCAAGGACATTGACGTGTCTGTCGAAAAAGAAAAACCTGGGTCCCC GGCAGTGACATTGCTGATCCGCAACCCCGAGGAGATTAGTGTCGACATTATTCTTGCGCTGGA GTCCAAGGGAAGTTGGCCCATCTCTACCAAGGAAGGACTTCCTATCCAGGGATGGCTTGGAAC CAAAGTTCGTACGAACTTACGCCGTGAGCCATTCTACTTAGTCCCAAAAAACGCGAAAGACGGA AATAGCTTTCAAGGGGAAACCTGGCGCTTATCGTTCTCTCACACGGAAAAATACATTCTGAATAA CCATGGAATCGAAAAGACATGTTGTGAATCTTCCGGTGCCAAATGCTGCCGCAAAGAATGTTTG AAATTAATGAAGTACTTACTGGAGCAGCTTAAAAAGGAGTTCCAAGAATTAGACGCGTTTTGTTC CTACCACGTTAAAACAGCGATCTTCCATATGTGGACTCAAGATCCTCAAGACAGTCAATGGGAC CCCCGCAATTTGTCGAGTTGCTTCGACAAATTACTTGCCTTCTTCTTAGAATGCCTGCGCACTGA GAAGTTGGATCATTATTTCATCCCCAAGTTTAATTTGTTCTCGCAAGAGTTGATTGATCGTAAATC CAAGGAGTTCTTGAGTAAAAAAATTGAGTACGAACGTAATAATGGATTTCCTATTTTTGACAAAC TGGACTACAAAGATCACGACGGGGACTACAAAGACCACGATATTGACTACAAAGATGATGACGA CAAAGATTACAAAGACGATGATGATAAAGATTATAAGGACGACGACGATAAATGAGAATTCATC G	pET28a(+)-*cGAS*

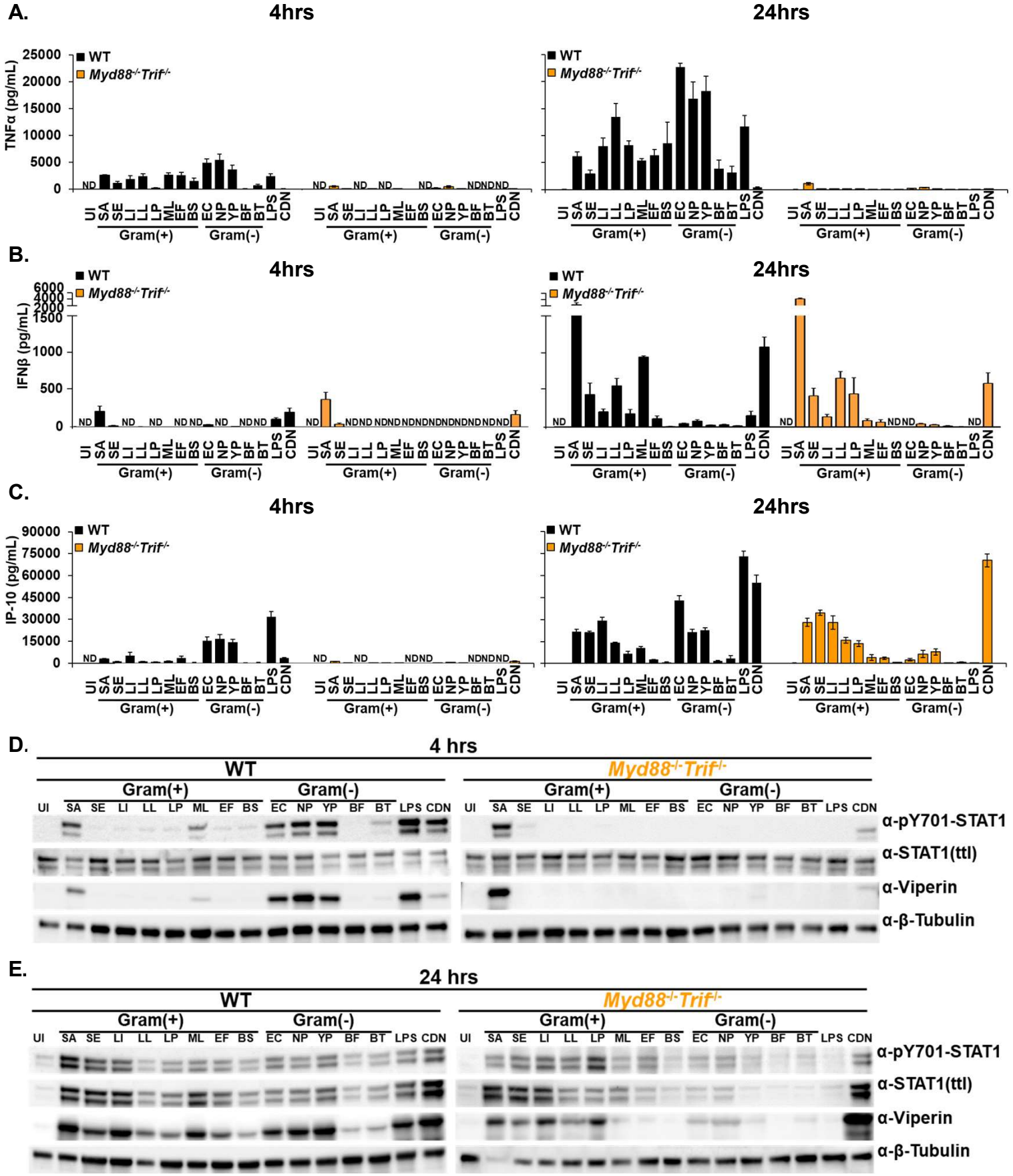
A.
4hrs
24hrs
TNFα (pg/mL)
WT
Myd88-/-Trif-/-
B.
IFNβ (pg/mL)
C.
IP-10 (pg/mL)
UI SA SE LI LL LP ML EF BS EC NP YP BF BT LPS CDN
Gram(+)
Gram(-)
D.
4 hrs
WT
Myd88-/-Trif-/-
α-pY701-STAT1
α-STAT1(ttl)
α-Viperin
α-β-Tubulin
E.
24 hrs

Figure 1. Gram-positive and Gram-negative bacteria stimulate IFN-I responses in macrophages with differing kinetics and reliance on TLR signaling.
WT and *Myd88*$^{-/-}$*Trif*$^{-/-}$ iBMMs were left untreated (uninfected, "UI") or exposed to LPS (1 µg/mL), 2'3'-c-di-AM(PS)2 (Rp, Rp) (herein, "CDN"; 1 µg/mL), and Gram-positive (Gram(+)) or Gram-negative (Gram(-)) bacteria at an MOI of 50. After 1 hr post-exposure, non-adherent, extracellular bacteria were removed and host membrane-impermeant antibiotics added to inactivate remaining bacteria. At 4 and 24 hrs post-exposure, conditioned supernatants were collected, followed by collection of protein from whole cell lysates. Conditioned supernatants were analyzed by ELISA for TNFα (**A**), IFNβ (**B**), and IP-10 (**C**) protein. Values represent the mean ± SEM of *n* = 3-12 biological replicates. Protein lysates were analyzed by immunoblot for phosphorylated STAT1 (pY701), total STAT1, Viperin, and β-Tubulin proteins at 4 hrs (**D**) and 24 hrs (**E**). Shown is 1 representative immunoblot of 3 independent experiments. Abbreviations: lipopolysaccharide ("LPS"), cyclic dinucleotide ("CDN"), *S. aureus* ("SA"), *S. epidermidis* ("SE"), *L. innocua* ("LI"), *L. lactis* ("LL"), *L. plantarum* ("LP"), *M. luteus* ("ML"), *E. faecalis* ("EF"), *B. subtilis* ("BS"), *E. coli* ("EC"), *N. perflava* ("NP"), *B. fragilis* ("BF"), *B. thetaiotaomicron* ("BT"), *Y. pseudotuberculosis* ("YP"), Not Detected ("ND").

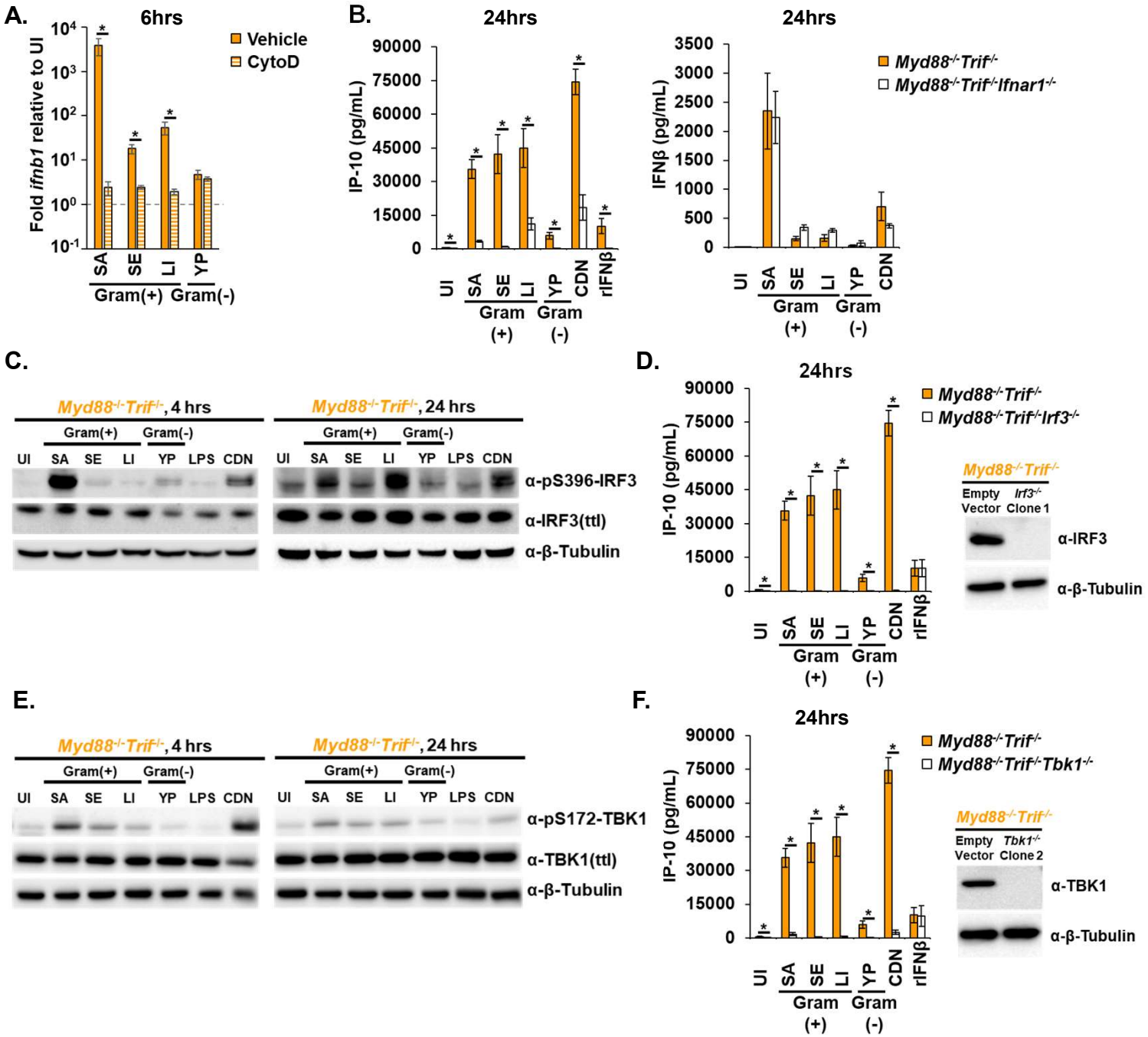
A.
6hrs
Vehicle
CytoD
Fold ifnb1 relative to UI
SA
SE
LI
YP
Gram(+)
Gram(-)
B.
24hrs
IP-10 (pg/mL)
UI
SA
SE
LI
YP
CDN
rIFNβ
Gram (+)
Gram (-)
24hrs
IFNβ (pg/mL)
Myd88-/-Trif-/-
Myd88-/-Trif-/-Ifnar1-/-
C.
Myd88-/-Trif-/-, 4 hrs
Myd88-/-Trif-/-, 24 hrs
Gram(+)
Gram(-)
UI
SA
SE
LI
YP
LPS
CDN
α-pS396-IRF3
α-IRF3(ttl)
α-β-Tubulin
D.
24hrs
IP-10 (pg/mL)
Myd88-/-Trif-/-
Myd88-/-Trif-/-Irf3-/-
Myd88-/-Trif-/-
Empty Vector
Irf3-/- Clone 1
α-IRF3
α-β-Tubulin
E.
Myd88-/-Trif-/-, 4 hrs
Myd88-/-Trif-/-, 24 hrs
α-pS172-TBK1
α-TBK1(ttl)
α-β-Tubulin
F.
24hrs
IP-10 (pg/mL)
Myd88-/-Trif-/-
Myd88-/-Trif-/-Tbk1-/-
Myd88-/-Trif-/-
Empty Vector
Tbk1-/- Clone 2
α-TBK1
α-β-Tubulin

Figure 2. TLR-independent IFN-I responses to bacteria in macrophages require IFNAR, IRF3, and TBK1.
A. *Myd88*$^{-/-}$*Trif*$^{-/-}$ iBMMs were pretreated with cytochalasin D ("CytoD", 10µg/mL) for 10min prior to and throughout exposure to Gram-positive (Gram(+)) or Gram-negative (Gram(-)) bacteria at an MOI of 50. After 6 hrs exposure, RNA was collected and *ifnb1* transcript abundance analyzed with respect to the *tbp* internal control. Data are expressed as the fold change relative to uninfected control (set to 10^0).
B. *Myd88*$^{-/-}$*Trif*$^{-/-}$ and *Myd88*$^{-/-}$*Trif*$^{-/-}$*Ifanr1*$^{-/-}$ iBMMs were left untreated ("UI") or exposed to CDN (1 µg/mL), recombinant IFNβ ("rIFNβ", 50ng/mL), and bacteria at an MOI of 50. After 1 hr post-exposure, non-adherent, extracellular bacteria were removed and host membrane-impermeant antibiotics added to inactivate remaining bacteria. At 24 hrs, supernatants were collected and analyzed by ELISA for IP-10 (left) and IFNβ (right).
C. *Myd88*$^{-/-}$*Trif*$^{-/-}$ iBMMs were left untreated (uninfected, "UI") or exposed to LPS (1µg/mL), CDN (1µg/mL), and bacteria at an MOI of 50 and treated with antibiotics as in Fig. 2B. At 4 and 24 hrs post-exposure, protein from whole cell lysates was collected and analyzed by immunoblot for phosphorylated IRF3 (pS396), total IRF3, and β-Tubulin proteins.
D. *Myd88*$^{-/-}$*Trif*$^{-/-}$ and *Myd88*$^{-/-}$*Trif*$^{-/-}$*Irf3*$^{-/-}$ iBMMs were treated as in Fig. 2B, and 24 hr supernatants were collected and analyzed by ELISA for IP-10. Whole cell lysates from *Myd88*$^{-/-}$*Trif*$^{-/-}$ and *Myd88*$^{-/-}$*Trif*$^{-/-}$*Irf3*$^{-/-}$ iBMMs were also analyzed by immunoblot for IRF3 and β-Tubulin proteins.
E. *Myd88*$^{-/-}$*Trif*$^{-/-}$ iBMMs were treated as in Fig. 2C. Protein lysates were analyzed by immunoblot for phosphorylated TBK1 (pS172), total TBK1, and β-Tubulin proteins.
F. *Myd88*$^{-/-}$*Trif*$^{-/-}$ and *Myd88*$^{-/-}$*Trif*$^{-/-}$*Tbk1*$^{-/-}$ iBMMs were treated as in Fig. 2B. Immunoblots were analyzed for TBK1 and β-Tubulin proteins.
Values represent the mean ± SEM of n = 3-6 biological replicates; *$p \leq 0.05$ student's *t*-test. Abbreviations: lipopolysaccharide ("LPS"), cyclic dinucleotide ("CDN"), *S. aureus* ("SA"), *S. epidermidis* ("SE"), *L. innocua* ("LI"), and *Y. pseudotuberculosis* ("YP").

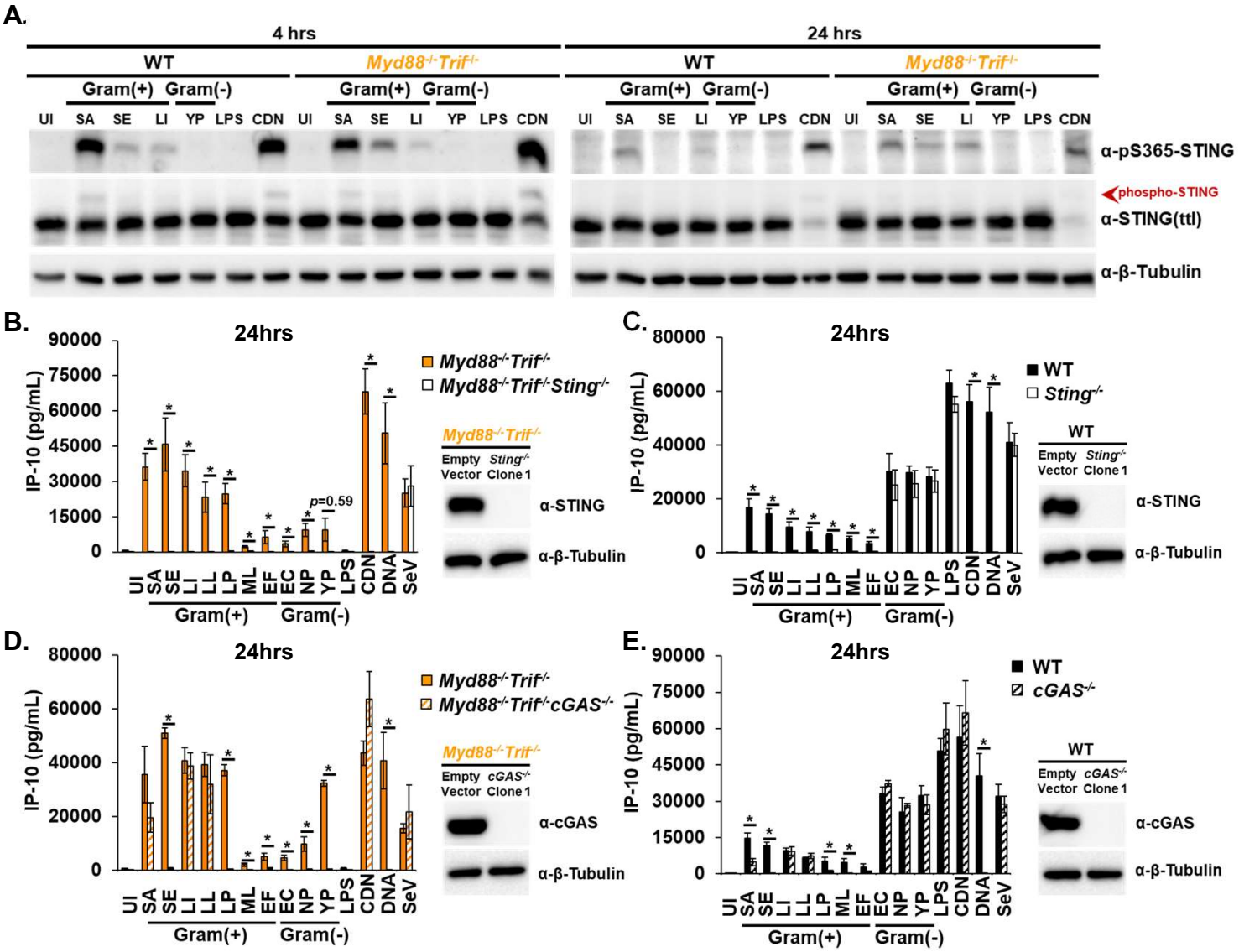

Figure 3. STING controls TLR-independent IFN-I responses to bacteria in macrophages.

A. WT and *Myd88*$^{-/-}$*Trif*$^{-/-}$ iBMMs were left untreated (uninfected, "UI") or exposed to LPS (1 µg/mL), CDN (1µg/mL), and Gram-positive (Gram(+)) or Gram-negative (Gram(-)) bacteria at an MOI of 50. After 1 hr exposure, non-adherent, extracellular bacteria were removed and host membrane-impermeant antibiotics added to inactivate remaining bacteria. At 4 and 24 hrs post-exposure, whole cell lysates were collected and protein analyzed by immunoblot for phosphorylated STING (pS365), total STING, and β-Tubulin proteins. Shown is 1 representative immunoblot of 3 independent experiments.

B. *Myd88*$^{-/-}$*Trif*$^{-/-}$ and *Myd88*$^{-/-}$*Trif*$^{-/-}$*Sting*$^{-/-}$ iBMMs were treated as in Fig. 3A with addition of cytosolically-delivered DNA (1µg/mL) and Sendai Virus ("SeV", MOI of 0.00001). At 24 hrs post-exposure, conditioned supernatants were collected and analyzed by ELISA for IP-10. Whole cell lysates from *Myd88*$^{-/-}$*Trif*$^{-/-}$ and *Myd88*$^{-/-}$*Trif*$^{-/-}$*Sting*$^{-/-}$ iBMMs were analyzed by immunoblot for STING and β-Tubulin proteins.

C. WT and *Sting*$^{-/-}$ iBMMs were treated as in Fig. 3B. Immunoblots were analyzed for STING and β-Tubulin proteins.

D. *Myd88*$^{-/-}$*Trif*$^{-/-}$ and *Myd88*$^{-/-}$*Trif*$^{-/-}$*cGAS*$^{-/-}$ iBMMs were treated as in Fig. 3B. Immunoblots were analyzed for cGAS and β-Tubulin proteins.

E. WT and *cGAS*$^{-/-}$ iBMMs were treated as in Fig. 3B. Immunoblots were analyzed for cGAS and β-Tubulin proteins.

Values represent the mean ± SEM of n = 3-12 biological replicates; *$p \leq 0.05$ student's t-test. Abbreviations: lipopolysaccharide ("LPS"), cyclic dinucleotide ("CDN"), *S. aureus* ("SA"), *S. epidermidis* ("SE"), *L. innocua* ("LI"), *L. lactis* ("LL"), *L. plantarum* ("LP"), *M. luteus* ("ML"), *E. faecalis* ("EF"), *E. coli* ("EC"), *N. perflava* ("NP"), and *Y. pseudotuberculosis* ("YP").

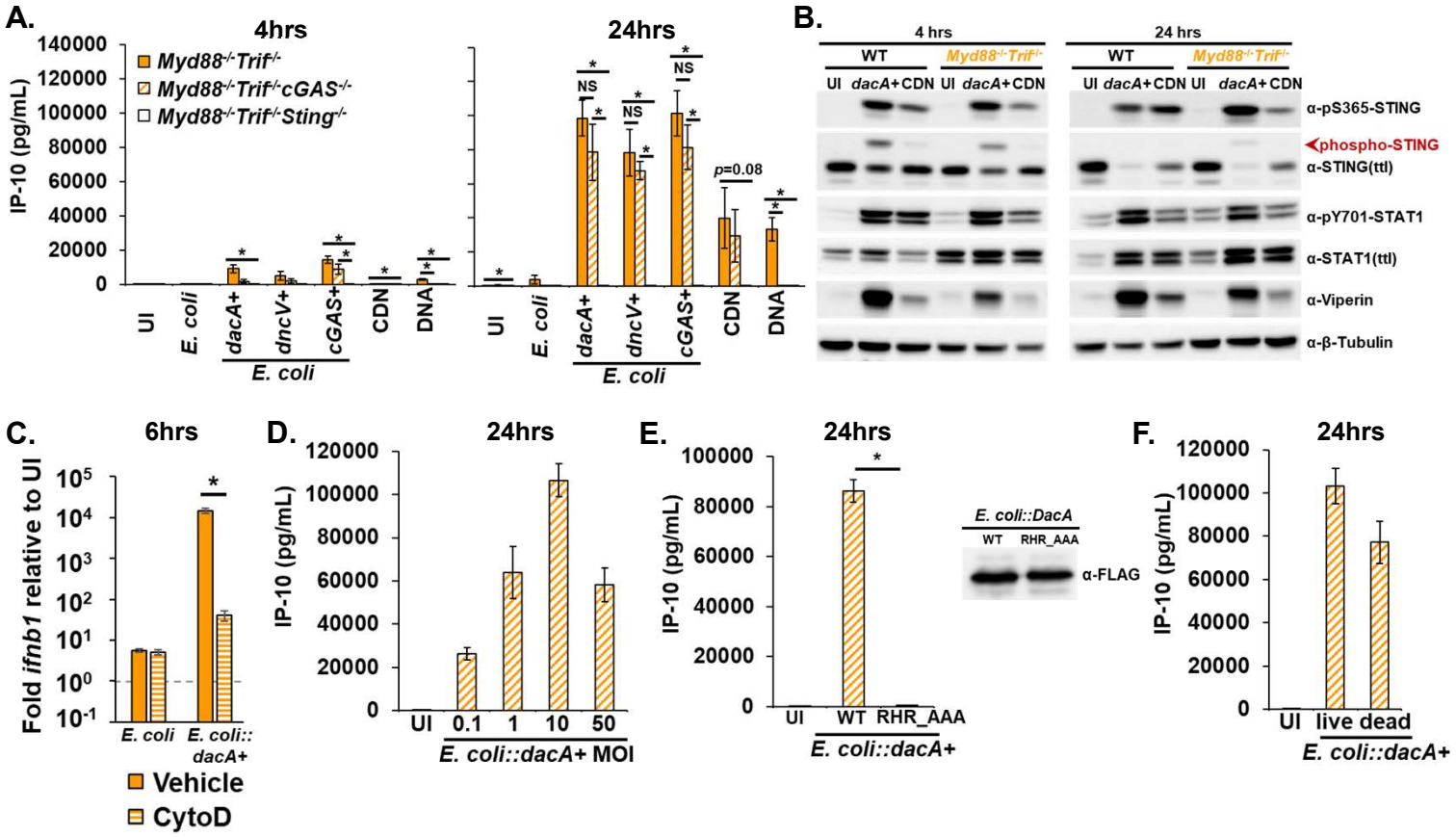

Figure 4. CDN synthesis in *E. coli* is sufficient to dictate cGAS-independent, STING-dependent IFN-I responses to bacteria in macrophages.

A. *E. coli* were treated with 1mM IPTG to induce expression of *dacA*, *dncV*, or *cGAS* for 3 hrs prior to infection. *Myd88*$^{-/-}$*Trif*$^{-/-}$, *Myd88*$^{-/-}$*Trif*$^{-/-}$*cGAS*$^{-/-}$, and *Myd88*$^{-/-}$*Trif*$^{-/-}$*Sting*$^{-/-}$ iBMMs were left untreated (uninfected, "UI") or exposed to cyclic dinucleotide (1µg/mL, "CDN"), cytosolically-delivered DNA (1µg/mL), and bacteria at an MOI of 50. After 1 hr exposure, non-adherent, extracellular bacteria were removed and host membrane-impermeant antibiotics added to inactivate remaining bacteria. At 4 (left) and 24 (right) hrs post-exposure, conditioned supernatants were collected and analyzed by ELISA for IP-10.

B. WT and *Myd88*$^{-/-}$*Trif*$^{-/-}$ iBMMs were exposed to 0.01mM IPTG-induced *E. coli::dacA*+ as in Fig. 4A. At 4 and 24 hrs post-exposure, whole cell lysates were collected and protein analyzed by immunoblot for phosphorylated STING (pS365), total STING, phosphorylated STAT1 (pY701), total STAT1, Viperin, and β-Tubulin proteins.

C. *Myd88*$^{-/-}$*Trif*$^{-/-}$ iBMMs were treated with CytoD as in Fig. 2A and then exposed to 1mM-IPTG-treated *E. coli* and *E. coli::dacA*+ as in Fig. 4A. After 6 hrs exposure, RNA was collected and *ifnb1* transcript abundance analyzed with respect to the *tbp* internal control. Data are expressed as the fold change relative to UI control (set to 10^0).

D. *Myd88*$^{-/-}$*Trif*$^{-/-}$*cGAS*$^{-/-}$ iBMMs were exposed to 1mM IPTG-induced *E. coli::dacA*+ at increasing MOIs as in Fig. 2A. At 24 hrs post-exposure, conditioned supernatants were collected and analyzed by ELISA for IP-10.

E. *Myd88*$^{-/-}$*Trif*$^{-/-}$*cGAS*$^{-/-}$ iBMMs were exposed to 1mM IPTG-induced *E. coli::dacA*$_{WT}$+ and *E. coli::dacA*$_{RHR_AAA}$+ (which were harvested for bacterial whole cell lysates and analyzed by immunoblot for FLAG protein expression) as in Fig. 4A. At 24 hrs post-exposure, conditioned supernatants were collected and analyzed by ELISA for IP-10.

F. *E. coli::dacA*+ were treated with 1mM IPTG as in Fig. 4A and then left untreated ("live") or treated with paraformaldehyde for 15 min ("dead"). *Myd88*$^{-/-}$*Trif*$^{-/-}$*cGAS*$^{-/-}$ iBMMs were then exposed to bacteria as in Fig. 4A. At 24 hrs post-exposure, conditioned supernatants were collected and analyzed by ELISA for IP-10.

For immunoblots, shown are 1 representative immunoblot of 3 independent experiments. Values represent the mean ± SEM of n = 3-6 biological replicates. *$p \leq 0.05$, student's t-test. NS, not significant.